J Fluoresc (2010) 20:1139–1157
DOI 10.1007/s10895-010-0665-6

INVITED REVIEW ARTICLE

Fluorescence Techniques for Determination of the Membrane Potentials in High Throughput Screening

Magda Przybylo · Tomasz Borowik · Marek Langner

Received: 15 February 2010 / Accepted: 5 April 2010 / Published online: 14 April 2010

Abstract The characterization of small molecules requires identification and evaluation of several predictive parameters, when selecting compounds for pharmacological applications and/or determining their toxicity. A number of them are correlated with the compound interaction with biological membranes and/or capacity to cross them. The knowledge of the extent of adsorption, partition coefficient and permeability along with the compound ability to alter membrane properties are critical for such studies. Lipid bilayers are frequently used as the adequate experimental models of a biological membrane despite their simple structure and a limited number of components. A significant number of the biologically relevant lipid bilayer properties are related to its electrostatics. Three electrostatic potentials were defined for the lipid bilayer; the intrinsic or induced surface electrostatic potential, the dipole potential and the membrane potential. Each of them was measured with dedicated methodologies. The complex measurement protocols and technically demanding instrumentation made the development of efficient HTS approaches for complete characterization of membrane electrostatics practically impossible. However, the rapid development of fluorescence techniques accompanied by rapid growth in diversity and number of dedicated fluorescent probes enabled characterization of lipid bilayer electrostatics in a moderately simple manner. Technically advanced, compact and automated workstations, capable of measuring practically all fluorescence parameters, are now available. Therefore, the proper selection of fluorescent probes with measuring procedures can be designed to evaluate drug candidates in context of their ability to alter membrane electrostatics. In the paper we present a critical review of available fluorescence methods, useful for the membrane electrostatics evaluation and discuss the feasibility of their adaptation to HTS procedures. The significance of the presented methodology is even greater considering the rapid growth of advanced drug formulations, where electrostatics is an important parameter for production processes and pharmacokinetics of the product. Finally, the potential of the membrane electrostatics to emerge as a viable pharmacological target is indicated and fluorescence techniques capable to evaluate this potential are presented.

Keywords Fluorescence · Membrane electrostatic potential · HTS · Lipid bilayer

Magda Przybylo and Tomasz Borowik Both authors contributed equally

M. Przybylo (✉) · T. Borowik · M. Langner
Laboratory for Biophysics of Macromolecular Aggregates,
Institute of Biomedical Engineering and Measurements,
Wroclaw Technical University,
Pl. Grunwaldzki 13,
Wroclaw, Poland
e-mail: magdalena.przybylo@pwr.wroc.pl

T. Borowik
e-mail: tomasz.borowik@pwr.wroc.pl

M. Langner
e-mail: marek.langner@pwr.wroc.pl

Introduction

Electrostatic interactions are universally present in biological systems [1, 2]. Practically, all biological macromolecules pose non-uniform charge distribution, which affects their inter-and intra-molecular arrangement and stability whereas charged surfaces control spatial distribution of charged compounds within the various cellular compartments [3–6]. In addition, all biological processes take place in the complex solutions, which may affect electrostatic

interactions by screening charges and altering local water activity [6–9]. The contribution of electrostatic interactions in receptor-ligand association is accounted for in binding assays, but the effect of electrostatics associated with supramolecular structures requires different approaches. The charged surfaces alter concentrations of adjacent solutes, association, trans-membrane transport, trans-membrane potential generation/dissipation and functioning of the membrane-associated proteins [10–14]. Due to the complexity of the biological membranes, experimental studies were performed on various models, which were designed to mimic important biological membrane properties. Among them the lipid bilayer is the most popular. Its wide application results from the assumption that the lipid fraction of the biological membrane determines its electrical and barrier properties [15, 16]. Even in such simplified model, the spatial charge distribution together with charge fluxes across the membrane results in the complex electrostatic potential profile as schematically illustrated on Fig. 1 [3, 5, 15, 17]. This potential profile depends on both, the intrinsic membrane charge distribution (types of lipids, protein and carbohydrates) and the overall environmental context (electrochemical potential differences, ionic strength, ion types and pH) [18, 19].

Historically, three membrane potentials were defined; the trans-membrane potential difference ($\Delta\Psi$), the dipole potential (Ψ_d) and the surface potential (Ψ_s) [2, 3, 5, 15, 17, 20]. In reality, the electric field across the lipid bilayer has a continuous profile without clear distinction between the three potentials. However, specific potentials may be assigned to different membrane regions, i.e. the surface potential in the aqueous phase adjacent to the lipid bilayer surface, the dipole potential in the lipid bilayer interface and the trans-membrane potential in the lipid bilayer hydrophobic core (see Fig. 1).

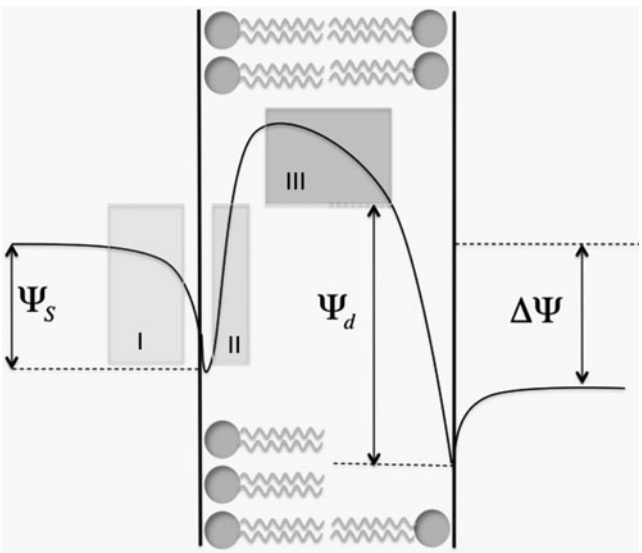

Fig. 1 The electrostatic potential profile across the lipid bilayer with the locations of fluorescent probes used to determine surface potential (area I), dipole potential (area II) and membrane potential difference (area III)

The trans-membrane potential difference ($\Delta\Psi$) is defined as the potential difference, generated by the transfer of charges, between two water compartments separated by the membrane. It is a critical parameter assigned to cell membranes and is frequently used as an indicator of cellular metabolic activity [19, 21]. It is also important for characterization of the cellular processes, such as mitochondria initiated apoptosis [22, 23]. The surface electrostatic potential (Ψ_s) is generated by charged lipid residues and/or charged compounds adsorbed within the membrane interface. It is defined as the potential in the aqueous phase adjacent to the membrane surface, which depends on the surface charge density and the ionic composition of the aqueous phase (for a review see [3, 5, 24]). In biological membranes, this potential is of the order of few tens of mV and may affect the surface related processes including conductance of ion channels [25–29], structure of membrane associated proteins [2, 30–33], binding of charged amphiphilic molecules [34] and sorting of charged lipids on the membrane surface [13]. The surface potential changes induced by adsorbed charged molecules affect the lipid head-group organization as shown for charged amphiphiles [35, 36] and some general anesthetics [37–39].

The surface membrane potential (Ψ_s) determines the distribution of ions at the membrane interface creating specific local ionic and pH environment. The ion concentration at the charged surface is described by the Boltzmann equation [3, 5]:

$$C_s = C_B \exp\left(\frac{-ze\Psi_S}{kT}\right), \tag{1}$$

where C_B and C_s are an ion concentrations at the membrane surface and in the bulk, respectively, e stands for elementary charge, k for Boltzmann constant, T for absolute temperature and z for ion valance. The surface electrostatic potential can be correlated with the surface charge density via the combination of the Poisson equation, which relates the electrical field vector to the surface charge density *(σ),* the Boltzmann equation and suitable boundary conditions, yielding:

$$\sinh\left[\frac{e\Psi}{kT}\right] = \frac{1}{\sqrt{8N\varepsilon_r\varepsilon_0 kT}}\sigma\sqrt{CN_B}, \tag{2}$$

where N is the Avogadro number and CN_B the effective bulk ion concentration. This equation shows that any change in the ion concentration (or its valance) in the bulk phase results in change of the surface potential even when the surface charge density remains constant. The other important effect of the surface membrane charge is an

alteration of the local pH, which affects the protonation of the surface located residues. This important effect is usually represented by the combination of Boltzman relation in a logarithmic form and the Henderson-Hasselbalch equation:

$$\log\left[\frac{H_S^+}{H_B^+}\right] = 0.059\Psi, \tag{3}$$

$$pK_S = pK_B - \Psi, \tag{4}$$

where H_S^+ is the concentration of protons at the surface and H_B^+ in the bulk phase. However, a certain amount of caution is needed when the effect of ions on surface potential is considered. A number of recent experiments and computer simulations show that the value of ion charge is not the only determinant of its screening potency but also the ion size and level of its hydration [40].

The dipole potential drops across a small distance within the head-group region of the membrane, therefore the electric field strength produced is large reaching 10^8–10^9 Vm^{-1}. In comparison, a total membrane potential difference, $\Delta\Psi$, of 100 mV across a membrane of thickness 4 nm would result in the field strength across the whole membrane of the order of 10^7 Vm^{-1}. Unlike the surface potential, the dipole potential (Ψ_d) is independent of the ionic strength since it is the electrical potential within phospholipid membrane itself. It arises from the alignment of water dipoles adjacent to the membrane, ions associated with the interface, the polar head groups residual charges (from P-O-N dipoles and from the P-O bonds of phosphate groups), the ester bonds between alkyl chains and the lipid glycerol backbone [17, 40–52]. The estimates of the absolute Ψ_d values for phosphatidylcholine bilayers vary from ≈ 280 mV, as experimentally determined from the penetration rates of hydrophobic ions, to ≈ 500 mV, as computed from molecular dynamic simulation data and it is always positive in the membrane interior [48, 53]. As a result, the difference in the penetration rates between positively and negatively charged, structurally similar, hydrophobic ions reaches up to 6 orders of magnitude [2, 54–58]. The dipole potential is thus likely to have a great significance in affecting passive transport, controlling the conformation of ion-translocating membrane proteins and regulating of surface associated enzyme functions. It has been shown for example, that it affects the conductance of the gramicidin channel [59, 60], membrane adsorption, folding and insertion of amphiphilic peptides and proteins [61, 62], phospholipase A_2 activity [63], mitochondria functioning by influencing redox reactions kinetics [64–66] and the Na,K-ATPase activity [67]. It may also affect processes assigned to lipids themselves, including skin permeability [62], membrane fusion [68], action of anesthetics [50–52], the modulation of molecule-membrane interactions in lipid rafts with possible effects on cell signaling [62, 69, 70] and the membrane salvation [71, 72].

Membranes are structural elements of cells which participate in practically all their physiological events, including the energy transformation, the control of fluxes between cell inner space and its environment and information sorting and transduction [73]. Therefore, understanding the effect of biologically active compounds or aggregates on membrane structure and functioning is important for applied life sciences [74–78].

When developing and testing biologically active compounds or supramolecular structures, it is necessary to determine their effect on crucial parameters of biological system. In addition, if the compound is intended to become a drug than it is important to establish the effect of biological structures on the compound spatial and temporal distribution within the tissue [78–81]. These effects will depend on the compound ability to interact with various cellular structures on its way to the molecular target. The compound physiological activity can be correlated with a set of parameters, which can be determined using dedicated model systems [82, 83]. Membrane electrostatic potentials are rarely used for that purpose because there have been no convenient, reliable and quantitative experimental protocols available and because biological membranes have not been considered as a viable pharmacological targets [84]. This has been changing recently due to the rapid development of the fluorescent spectroscopic and imaging techniques and subsequent identification of intracellular pharmacological targets [1, 74, 85–105].

In order to study the effect of a compound and/or an aggregate on electrical properties of biological systems a suitable experimental models were developed including molecular monolayers, model lipid membranes with or without reconstituted proteins, extracted biological membranes or whole cells [16, 73, 106–108]. Moreover, in order to monitor the electrostatic potential the various detection techniques were developed, as well. Historically, electrochemical, spectroscopic and electrophysiological methods have been widely used [21, 39]. Their applications were limited to the specific model systems and required complex instrumentation. Fluorescence techniques, in the course of the last two decades, have been shown to be extremely useful in variety of applications in biological, medical and life sciences [90, 109]. The potential for miniaturization, rapid data acquisition and continuously increasing number of probes and labeling protocols makes fluorescence techniques a leading experimental approach in life sciences [110, 111]. In this review we present, available fluorescence techniques providing information on membrane electrostatic potential and their capability to be adapted for highly efficient screening methodologies.

Determination of the surface electrostatic potential

The membrane surface electrostatic potential can be determined by measuring the zeta potential of a particulate suspension. However, only the overall charge can be calculated without accounting for its spatial distribution and/or screening by a variety of surface modifications and/or shape alterations. For example, the zeta potential of erythrocytes is negative, due to the charges associated with the glycocalyx, whereas the outer layer of the lipid bilayer is devoid of electrostatic charges [73]. In order to address this, dedicated, appropriately localized fluorescent probes were developed. They are capable to probe the local electrostatic properties at various locations within the aggregate. There are three basic fluorescence approaches to study the surface electrostatics in bio-membranes and their models;

1) The fluorescent probe re-location from the aqueous phase onto the membrane surface under the influence of the local electric fields accompanied by fluorescence change;
2) The fluorescence change of the surface located dye caused by ions dissolved in the adjacent aqueous phase;
3) The direct response of a ground and excited electronic states to the local electric field, resulting in the shifts of an absorption and/or an emission spectra (electrochromism).

There is a number of charged amphiphilic fluorescent probes which have moderate partition coefficient and fluorescence properties dependent on the polarity of the environment, preferentially with high quantum efficiency in low dielectric media. Examples of such probes are presented on Fig. 2.

When liposome suspension is labeled with such probe its fluorescence (F) will originate predominantly from the probe fraction located in the membrane, i.e.

$$F = \begin{cases} = 0 \quad for \quad C_{aq} \\ \approx f(C_{mem}) \quad for \quad C_{mem} \end{cases} \tag{5}$$

where C_{aq} and C_{mem} are the probe concentrations in the aqueous phase and the lipid bilayer, respectively. The apparent partition coefficient of the probe can be used to determine its surface concentration, modulated by the electrostatic potential as proposed by Eisenberg et al. [112]. Specifically, assuming that the intrinsic partition coefficient does not depend on the amount of surface electrostatic charge, one can write:

$$K^{app} = \frac{C_{mem}}{C_{aq}^{surf}} = \frac{C_{mem}}{C_{aq}^{bulk} \exp\left(\frac{-ze\Psi_S(z)}{kT}\right)} = \frac{K}{\exp\left(\frac{-ze\Psi_S(z)}{kT}\right)}, \tag{6}$$

where K^{app} is the ,experimentally determined, apparent partition coefficient for the charged membrane, whereas K is the intrinsic partition coefficient for a reference membrane without surface charges, i.e. formed from phosphatidylcholine. Since membrane associated fluorescent probes are practically the only source of fluorescence, the above equation can be rewritten as:

$$F^{charged} = \frac{C_{mem}}{C_{aq}^{surf}} = \frac{C_{mem}}{C_{aq}^{bulk} \exp\left(\frac{-ze\Psi_S(z)}{kT}\right)} = \frac{F^{neutral}}{\exp\left(\frac{-ze\Psi_S(z)}{kT}\right)}, \tag{7}$$

where $F_{charged}$ and $F_{neutral}$ represent fluorescence intensities obtained when the dye is exposed to the charged or

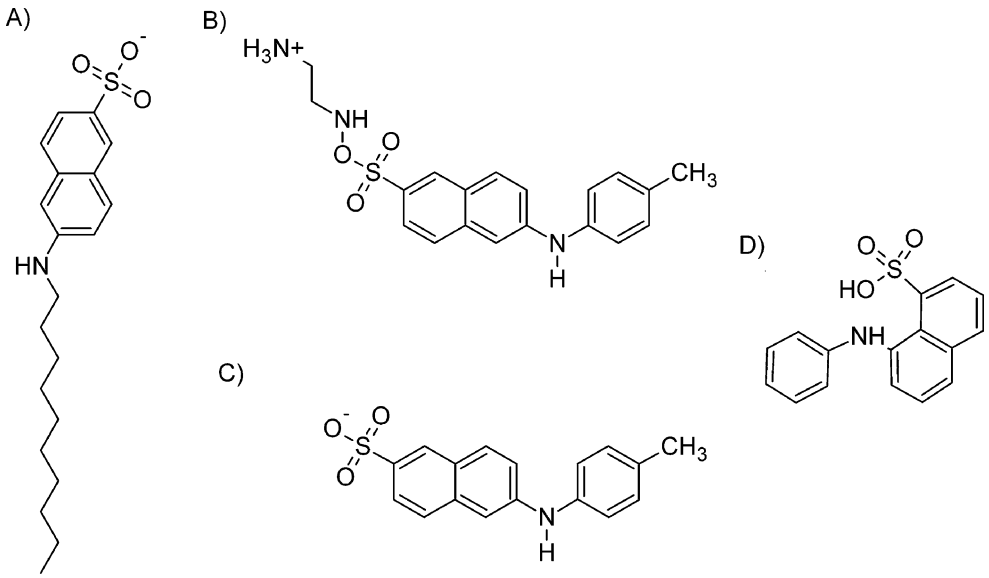

Fig. 2 Examples of charged fluorescent probes used to measure the surface electrostatic potential (**a**) Negatively charged 2-(hexadecylamino)naphthalene-6-sulfonate (HNS), (**b**) 1-anilinonaphthalene-8-sulfonic acid (1,8-ANS), (**c**) 2-p-toluidinylnaphthalene-6-sulfonate (TNS), (**d**) positively charged N-(β-aminoethyl)sulfonoamido derivative of TNS (TNAES)

neutral membranes, respectively. This approach was used to determine the experimental limitations of Gouy—Chapman theory. Specifically, two chemically similar, but oppositely charged fluorescent probes (Fig. 2) were used to determine the surface electrostatic potentials of lipid bilayers with various amount and types of phosphoinositides. It was established that when PIP_2 was present in the membrane the electrostatic potential determined with cationic probe did not correspond to that obtained with anionic probe. This result was interpreted as a surface electrostatic potential non-uniformity in the presence of PIP_2 [4], whereas when lipids with lower quantities of negative charges were used such effect was not observed. Using this method a care has to be taken to ensure the surface "quality", i.e. the lipid bilayer has to be far from any phase transitions [113].

The other method available is the quenching of a surface located fluorophore. The local charged quencher concentration depends on the local electrostatic potential according to the Boltzman relation:

$$C_s = C_B \exp\left(\frac{-ze\Psi_S(z)}{kT}\right), \tag{8}$$

where the local ion concentration (C_S) depends on the bulk concentration (C_B) and local electrostatic potential, $\Psi_s(z)$. Therefore, the fluorescent probe at a certain location is quenched with the efficiency correlated with a value of the local electrostatic potential. Specifically, the dynamic quenching is described by the Stern-Volmer Eq. 9 [114];

$$\frac{F_0}{F} = 1 + K_{SV}[Q]_{local}, \tag{9}$$

$$[Q]_{local} = [Q]_{bulkl} \exp\left(\frac{-ze\Psi_{local}(z)}{kT}\right), \tag{10}$$

where F_0 and F are fluorescence intensities in the absence and presence of a quencher, respectively. K_{SV} is the Stern-Volmer constant and $[Q]_{local}$ the local quencher concentration.

The graphical representation of the Stern-Volmer equation and the effect of a surface charge is illustrated on Fig. 3.

The determination of the electrostatic potential, in this case, consists of two steps; the measurement of an intrinsic quenching constant using a neutral model membrane (or neutral quencher) and the determination of apparent quenching constant when surface charges are present. The application of neutral quencher for the intrinsic quenching constant determination is preferred since in this case there is no need for an additional experiment to evaluate the effect of the surface charge on the dye location [4, 114, 115].

Since the value of the electrostatic potential depends on the probe location the proper dye positioning is

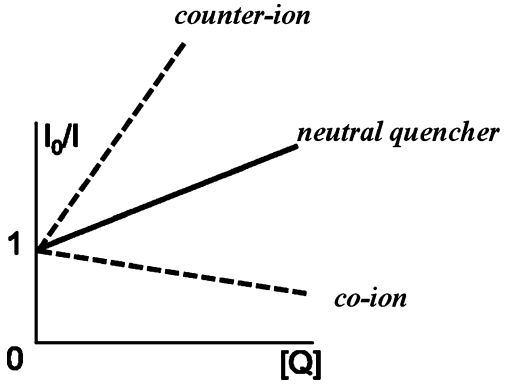

Fig. 3 The graphical representation of the Stern-Volmer equation for the quenching of surface located fluorophore. The solid line represents the case when the fluorophore is quenched with neutral water soluble quencher whereas the broken lines show the quenching of the fluorophore by counter-ionic and co-ionic quenchers

critical [5]. To ensure the correct probe location its physicochemical properties need to be selected carefully; otherwise the intended effect may not be achieved. For example, the attachment of NBD dye to the hydrocarbon chain of lipid does not result in expected fluorophore location. Amphiphilic NBD molecule has strong preference for the lipid bilayer interface and as a consequence it is positioned there despite the place of its attachment [116]. Therefore, it is a good practice to determine the fluorophore location in the independent experiment [117, 118]. The electrostatic potential determination using the dynamic quenching method was creatively used by McLaughlin group [4, 115]. The objective was to determine the electrostatic potential profile for various charged lipid bilayers [4, 119, 120]. For that purpose fluorescein located at 0 nm, 1 nm and 2 nm from the membrane surface,were used. To achieve that hydrophilic fluorescent moieties were attached to carefully selected lipid carriers; phosphatidylethanolamine with covalently attached fluorescein to the lipid headgroup (lipid bilayer surface - 0 nm); ganglioside GM1 with fluorophores attached to sialic acid (1 nm from the lipid bilayer surface) and at the terminal glucose (2 nm from the lipid bilayer surface) as illustrated on Fig. 4 [4, 5]. Using this approach it was possible to obtain the electrostatic potential profile for charged lipid bilayers [4, 119].

A similar strategy was proposed by Kraayenhof et al. [121, 122]. In this approach the combination of charged group and hydrocarbon chain defines the position of the 7-hydroxycoumarin probe with respect to the membrane surface. A short spacer between the quaternary ammonium group and the fluorophore was used to position the fluorescent group at a certain distance from the membrane surface. The usefulness of this strategy was demonstrated by measuring the fluorescent properties of a series of such

analogs in charged membranes and by monitoring the surface potential changes during metabolism in yeast cells [121]. Some of such probes were used to study the differential effects of monovalent cations on membrane surface properties [123]. Like in the previous example, the measured fluorescence properties of the probes were well correlated with the surface potential calculated from the Gouy-Chapman-Stern theory [121, 123]. (Figure 4)

The electrostatic potential in the aqueous phase adjacent to charged surface can also be measured by the extent of fluorescent probe protonation [124]. Due to its polarity, fluorescein attached to the lipid polar head-group stays above the membrane surface probing the water phase in its immediate vicinity. Fluorescein quantum yield depends on its protonation, being non-fluorescent in low pH. Therefore, the fluorescence intensity of fluorescein may be correlated

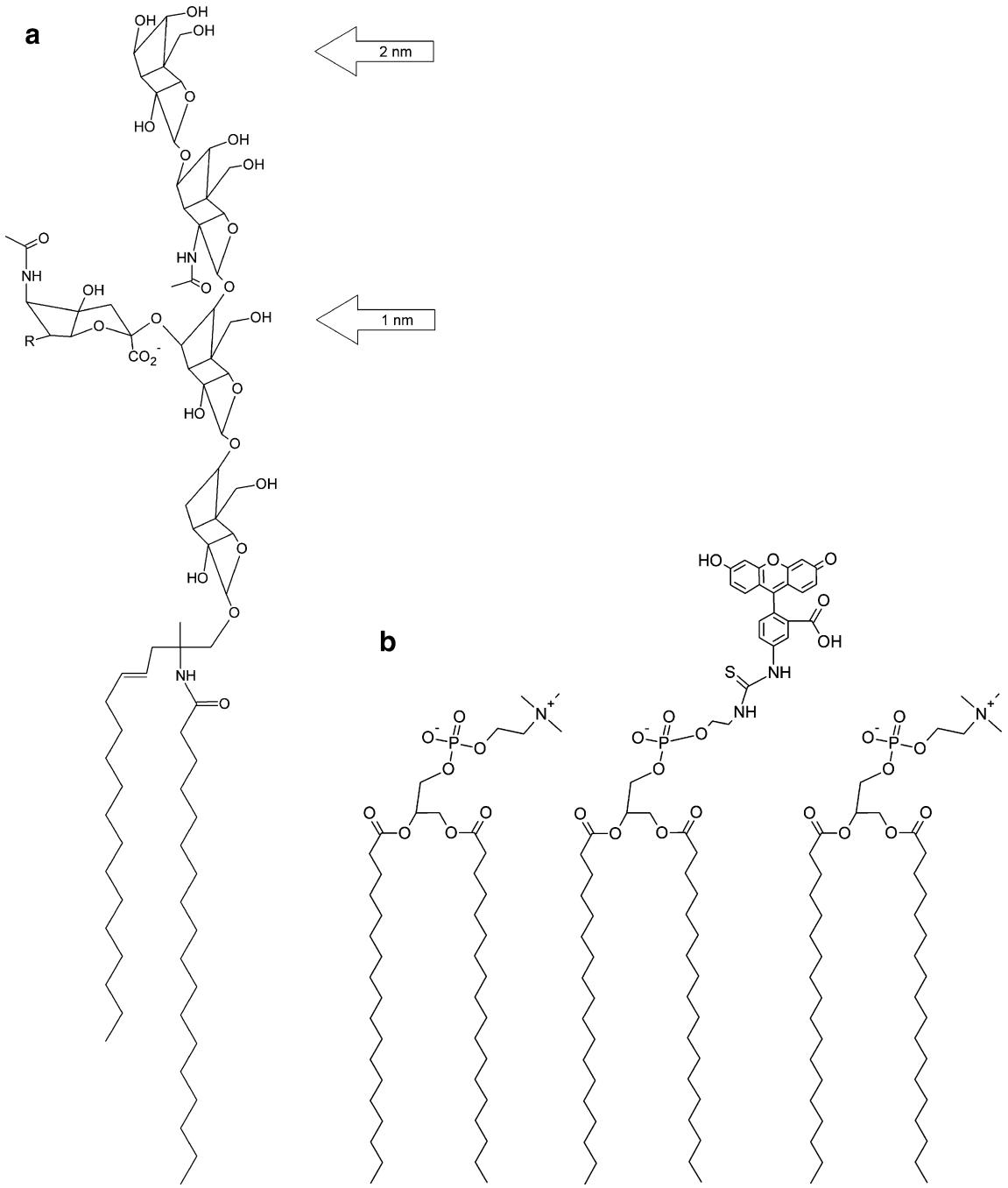

Fig. 4 The chemical structure of (**a**) ganglioside GM1 with indicated locations of fluorescence dyes and. (**b**) surface located fluorophore of N-(fluorescein-5-thiocarbamoyl)-1,2-dihexadecanoyl-sn-glycero-3-phosphoethanoloamine, triethylammonium salt (Fluorescein DHPE) dye

with the surface electrostatic potential of the membrane. Specifically, at a charged surface the apparent pK^{obs} of the surface located fluorescent probe can be correlated with the local electrostatic potential [124]:

$$pK^{obs} = pK^0 - \frac{F\Psi_S}{2.3kT}, \quad (11)$$

where pK^0 is the intrinsic pK when there are no surface charges present. The number has to be determined in the independent experiment under similar conditions. The calibration of the pK^{obs} versus surface potential, Ψ_s, can be done using, for example, POPC lipid bilayer as the neutral phospholipid surface and mixtures of POPC/DOPG with increasing fraction of charged lipid. Care needs to be taken to ensure that the charged component is randomly distributed on the lipid surface in order to avoid erroneous results [113]. Values of the fluorescent probe pK^{obs} are usually determined by fitting the fluorescence intensities as a function of the aqueous pH to the following formula:

$$pK^{obs} = pH - \log\left(\frac{\alpha}{1-\alpha}\right), \quad (12)$$

with $\alpha = (F - F_{AH+})/(F_A - F_{AH+})$, where F is the fluorescence intensity at the band maximum of the conjugate acid-base forms at the particulate pH being examined. F_{AH+} and F_A are the fluorescence intensities at the same wavelength at pH values such that only AH^+ or A exists. Similar approach was used to detect adsorption of charged molecules onto the lipid surface [125–128]. The lipid labeled with fluorescein has been recently employed as the detector in liposome based biosensor to determine the permeability coefficient of charged biologically active compounds [129–131].

The third and least frequently used approach for the surface potential determination takes advantage of the electrochromic effect, namely the electric field induced changes in electron or proton distribution within the fluorescence probe itself [109, 132–134]. However, application of such dyes has a number of serious disadvantages. Electrochromic dyes are usually large molecules; therefore it is impossible to determine their precise location within the lipid bilayer interface and consequently obtained value of the surface electrostatic potential cannot be precisely assigned to the specific location. Since those dyes are amphiphilic or hydrophobic it is impossible to determine the value of the electrostatic potential further than the membrane interface.

Using the fluorescent dyes to evaluate the surface electrostatic potential fluorophore size and/or charge has to be accounted for since they can modify the local lipid surface properties including the electrostatic potential by itself [135–137]. When measuring the surface electrostatic potential in biological membranes a number of intrinsic difficulties needs to be overcome, including their non-homogenous lateral organization and transversal asymmetry [138–147]. There are numerous problems with the labeling protocols of biological membranes due to the limited solubility of the dye, inhomogeneous distribution within the biological system and potential dye specificity towards membrane components. All those difficulties are irrelevant when not the electrostatic surface potential but the presence of charged lipids in certain location is to be determined; this was exemplified by fluorescent annexin-V conjugates used for studying the externalization of phosphatidylserine, one of the earliest indicators of apoptosis [148, 149]. The measured difference in fluorescence intensities of annexin-V-phosphatidylserine complexes between apoptotic and non-apoptotic cells can be detected by flow cytometry. The fluorescence signal is elevated by about 100-fold as illustrated by studies on a hybridoma cell lines with the annexin-V assay, used to study apoptosis and its suppression by bcl-2 over-expression [150, 151].

Determination of the dipole potential

The direct measurements of the dipole potential were possible by the application of phospholipid monolayers on air–water or water-mercury interfaces using ionizing electrodes. The value of the dipole potential for phosphatidylcholine was determined to be about 450 mV [37–39, 65]. However, results from monolayers disagree quantitatively with the dipole potential values obtained on the bilayer models using other methods, i.e. EPR [152] or NMR [43]. This causes serious difficulties with the calibration of the fluorescence methods for the dipole potential determination [153].

When a dye binds to the lipid membrane with its chromophore in the lipid headgroup region it is sensitive to the local electric field originating predominantly from the dipole potential as exemplified by styryl dyes (Fig. 5), which were primarily designed as fast-responding probes for transmembrane potential determination [48, 132, 154, 155].

There are three effects of the intra-membrane electric field on the membrane-bound dye molecules that could be used to quantify the dipole potential:

1. The pK_a of membrane-bound dye modification,
2. The fluorescence excitation and/or emission spectrum of membrane-bound dye shift,
3. The fluorophore relocation.

It has been shown that the pK_a of membrane-bound N-(4-Sulfobutyl)-4-(4-*p*-(dipentylamino)phenyl)butadienyl)-pyridinium inner salt (RH421) and 4-(2-(6-(dioctylamino)-2-

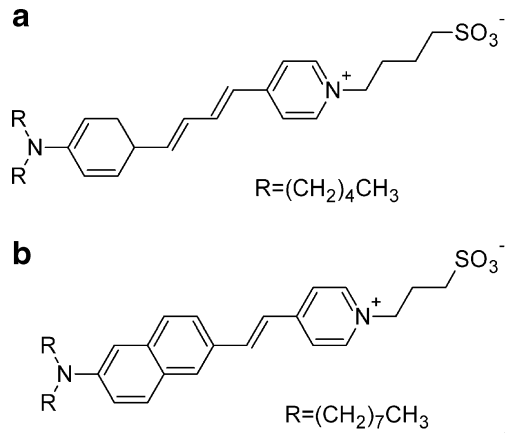

Fig. 5 Examples of two membrane dipole potential sensitive dyes: (**a**) RH 421 and (**b**) di-8-ANEPPS

naphthalenyl)ethenyl)-1-(3-sulfopropyl)-pyridinium inner salt (di-8-ANEPPS) depends on the structure of lipid used (i.e., chain length and saturation) [156, 157], when the dye is incorporated into dimyristoylphosphatidylcholine (DMPC) and dioleoylphosphatidylcholine (DOPC) membranes its pK_a is 3.1±0.1 and 4.1±0.1, respectively. The pK_a of such dyes can be determined by the large change in their absorbance (excitation) spectrum caused by the dye protonation. Although pK_a shift could be used to quantify the dipole potential, there are number of practical disadvantages of such method. It involves pH titrations down to the low, strongly acidic, pH values, i.e. at least pH 3 for RH421 and even lower for di-8-ANEPPS [156, 157]. Such titrations cannot be performed to pH values below 1.8 because of the protonation of the lipid phosphate group, resulting in the phase transition of the lipid aggregate [158–160]. Therefore, a method that involves measurements at a constant and physiological pH is preferable.

The convenient method can be based on the shift of the excitation and/or emission spectrum of the membrane-bound dye. Such application of di-8-ANEPPS dye was first proposed by Gross et al. [48], and shortly afterwards by Zouni et al. [156]. The binding of the dipolar species to the lipid bilayer, made of the neutral phosphatidylcholine, causes significant spectral shift of the dyes [48, 157] indicating their sensitivity to the local dipole potential. The response is based on the electrochromic effect (Stark effect) [134]. The effect is visualized by the shifts of the absorption and emission bands, caused by the interaction of the electric field (E) with the ground and excited states of chromophore dipole moments $\Delta\vec{\mu}$, as expressed by the equation [90, 134, 161]:

$$h\Delta\nu_{obs} = -\left(\frac{1}{\varepsilon_{ef}}\right)|\Delta\vec{\mu}||\vec{E}|\cos\theta, \qquad (13)$$

where $h\Delta\nu_{obs}$ is the spectral shift, θ – the angle between $\Delta\vec{\mu}$ and E vectors and ε_{ef} is a microscopic analog of dielectric constant (electric screening).

To achieve the optimal sensitivity of the dye to the dipole potential, a probe should exhibit two properties:

- substantial change of its dipole moment ($\Delta\vec{\mu}$) upon electronic excitation, i.e. a substantial redistribution of the electronic charge density,
- the probe should be located in nonpolar environment (ε_{ef} in the range of units) and oriented parallel or anti-parallel to the electric field (θ=0 or 180°).

Styryl dyes with electron-donor and electron-acceptor substituent at the opposite ends of the rod-shaped conjugated electronic systems are among the best known electrochromic dyes (Fig. 6). They exhibit strong excited state redistribution of the electronic charge that can be modulated by the electric field. For example, the 4-dialkylamino-3HFs are characterized by significant excited-state charge transfer occurring from its 4-dialkylamino to the 4-carbonyl group. In bio-membranes, the parallel orientation between the probe dipole and the dipole potential gradient can be achieved by design, in which probe charged groups are anchored to the lipid polar regions, and the rod-like chromophore is oriented perpendicular to the surface of the bilayer. Ideally the probe should be located at the maximal electric field gradient; i.e. on the level of the phospholipid carbonyl groups [154]. The dye penetration depth can be controlled by the hydrophobic-hydrophilic balance of the probe molecule, as illustrated by 3HF (3-hydroxyflavone) derivatives, where the positively charged anchor is not a part of the chromophore, and therefore the connecting spacer may be of a variable length. Probes with the opposite orientations of their dipole moments were designed. Their application in comparative studies may exclude spectroscopic effects which do not depend on probe dipole moment orientation, such as polarity or viscosity [132, 154].

In order to quantify the spectral shifts, ratiometric methods were designed, i.e. they determine the ratio, R, of the fluorescence intensities at two excitation wavelengths at fixed emission wavelength. A decrease in R thus represents a decrease in the dipole potential and, correspondingly, an increase in R represents an increase in the dipole potential [48]. Styrylpyridinium dyes like di-8-ANEPPS allow ratiometric recording of Ψ_D, if the sample can be excited with two different wavelengths. When lipid vesicles or biomembrane suspensions are used, as experimental systems, this possibility is easily provided by common spectrofluorimeters. In contrast, for microscopic studies of cells it would be more convenient to apply dyes with a ratiometric response in emission that could be adapted for multi-color imaging microscopes. Moreover, ratiometric measurements in emission eliminate distortions of data caused by photobleaching, variations in the probe loading and instrumental factors such as light source

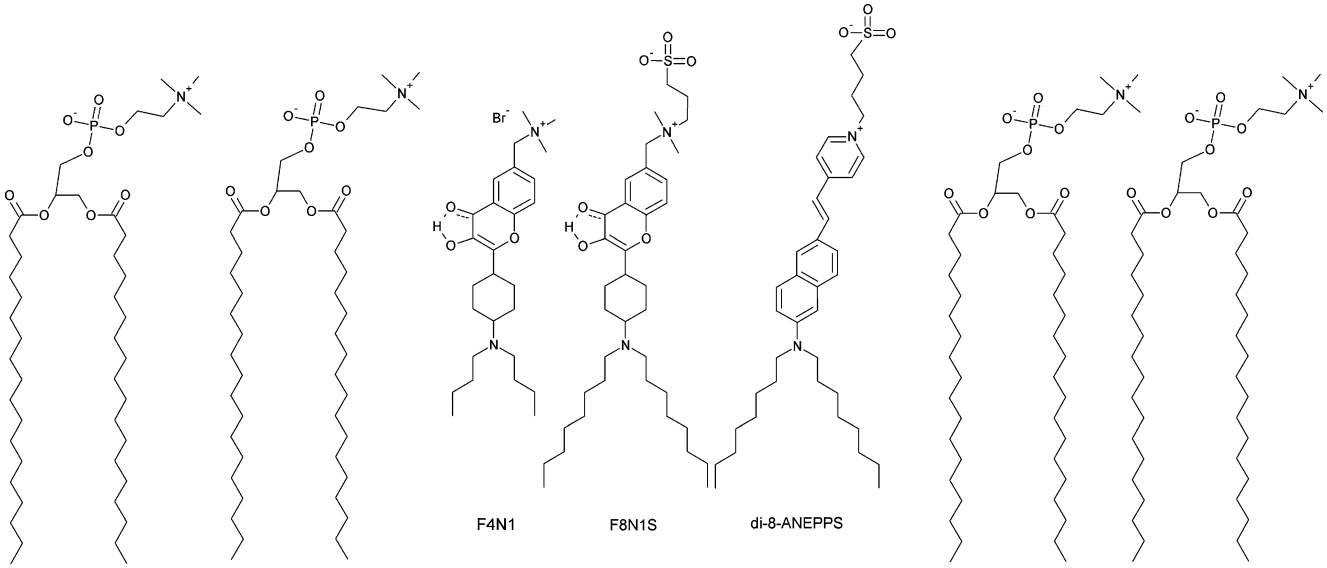

Fig. 6 Structure and estimated locations of F4N1, F8N1S and di-8-ANEPPS in a PC layer

stability. In this context, new fluorescent probes sensitive to the dipole potential were designed by using 3-hydroxyflavone (3-HF) derivatives. They exhibit two well-separated emission bands due to the presence of two forms in the excited state resulting from an excited state intra-molecular proton transfer [155]. The chemical structure and membrane location of 3-HF dyes is shown on Fig. 6.

Results from ratiometric and pK - alteration methods established that the value of the dipole potential decreases with increasing lipid chain saturation and, in the case of unsaturated lipids, with increasing length of the hydrocarbon chains. Both of these affect the spacing between headgroups, therefore modifying the dipole potential value [156, 157]. Dipole potential sensitive dyes were also used to investigate the effect of amphiphilic peptides and proteins on the dipole potential of lipid vesicles [61, 162–165], and to detect changes in local electric field associated with conformational changes of ion-translocating membrane proteins [63, 64]. A significant advantage of the ratiometric dyes over other methods is the possibility of using them to spatially resolve differences in the dipole potential over the surface of cells [153].

The dipole potential can be also measured with a relocation of a fluorescent dye attached to the lipid molecule [64]. When the DPPC bilayer was labeled with two fluorescent NBD moieties, covalently attached to the to the headgroup and to the acyl chain, both probes were sensitive to the dipole potential changes induced by the presence of phloretin and 6-ketocholestanol (6-KC) [154]. It is claimed that the two probes are detecting the dipole potential by the correlation between their fluorescence excitation shifts and the lipid packing density [157]. This approach is not widely used since the fluorescence change in this case intentionally depends on a combination of two effects; the dye location and the dipole potential change, which cannot be separated easily.

The *R*-value can be measured with up to 1% accuracy, so the effects of surface-active substances and the lipid structural changes on the dipole potential can be easily resolved. Unfortunately, the absolute determination of the dipole potential value by this method still relays on calibration with methods, which are considerably less accurate than the fluorescence measurements themselves [38, 43, 50, 55]. In principle, the calibration of the dyes might be possible by theoretical means, if the fluorescence excitation spectrum of the dye could be quantum mechanically calculated, the site and the orientation of the dye in the membrane were accurately known and the influence of the local field strength on the dye in the membrane could be determined [153]. The other approach used to calibrate the fluorescence measurements is the application of molecules known to modify the dipole potential, i.e. phloretin—the compound strongly reducing the dipole potential and sterols, ether phospholipids and especially 6-ketocholestanol (6-KC) which increase the dipole potential [72, 166]. Comparing the *R* values with Ψ_D values, obtained from kinetic measurements of hydrophobic ion transport across lipid bilayers, at different concentrations of phloretin and 6-KC [152], it was found that they are linearly correlated, i.e. a change of *R* of 0.8 corresponds to a change in Ψ_D of about 100 mV [48, 156]. Similarly, comparison of the *R*-values with packing densities, expressed as a surface area per lipid molecule (A), obtained with X-ray crystallography, for a number of

different lipids yielded an approximately linear correlation. This is consistent with the Helmholtz equation:

$$\Psi_d = \frac{\mu_\perp}{A\varepsilon_0\varepsilon}, \tag{14}$$

where $\mu_\perp$ is the average component of the lipid molecular dipole moment, including membrane-associated water molecules perpendicular to the plane of the membrane, ε_o is the permittivity of free space, and ε is the local dielectric constant [51].

When measuring dipole potential using fluorescent dyes, it is necessary to ensure that they are not sensitive to any other changes in the membrane physical properties. It has been shown that the membrane order in particular affects the fluorescence of membrane-bound RH421 and di-8-ANEPPS [153]. Sensitivity of the probes to the membrane order depends on the lipid used and on the emission wavelength chosen for the measurement. The origin of the fluidity-induced wavelength shifts of the probes can be attributed to the processes in the excited state. This could involve the conformational change of the dye molecular structure and a simultaneous reorganization of the dye solvatation shell. The effect can by completely excluded by measuring the fluorescence emission on the long wavelength red edge of the spectrum. The average fluorescence lifetime of red-edge emission is significantly longer than that on the blue edge, e.g. for RH421 in DMPC vesicles lifetime increases from 0.6 ns at 569 nm to 1.9 ns at 715 nm [157].

In addition, the probe can affect the outcome of the experiment by itself. In order to sense the electric field strength within the membrane the fluorophore must be charged. Therefore, the influence of the dyes on the intramembrane field strength cannot be avoided. It has been shown that the binding of RH421 to the lipid bilayer induces an increase in the positive dipole potential and in the rate constant of hydrophobic anion translocation through the membrane, due to the positive charge on its chromophore [135]. Consistently with these results, it was found that the increase in the surface density of RH421 and di-8-ANEPPS in DMPC vesicles causes the increase in the *R*-value,which can be related to the increase in the dipole potential. Titrations of RH421 and di-8-ANEPPS with lipid vesicles showed, however, that the dye-induced shift of the fluorescence excitation spectrum become negligible at a molar ratio of lipid to dye of > 200 [157].

The determination of the trans-membrane potential

Due to its importance, the trans-membrane potential has been a subject of intense research [19, 21, 73, 87]. Experimental methodologies were developed but most of them were designed for dedicated experimental models, therefore limiting the scope of their applications. By introducing fluorescence techniques to the common physiological and biophysical methods, experimental possibilities expanded enormously including both: studies on model and life systems. It was possible to monitor the kinetics of chemically and/or physically induced processes on excitable membranes [32, 87], to measure large cell populations with Fluorescence Assisted Cell Sorter (FACS) or Coultier-type counters [167–169], and even follow single cell events using various types of fluorescence microscopes [86, 89, 90, 111, 170, 171]. In addition, the combination of the fluorescence microscopy with single cell handling techniques opened new era in cell physiology studies [172–175] and made cell-based HTS techniques feasible [176–178].

The most popular fluorescent dyes used as trans-membrane potential probes, classified according to their chemical structure, include rhodamines [179–181], cyanines [182, 183], merocyanines [184] and oxonols [185]. From the functional point of view, they can be divided into fast and slow responding probes. Detection of the trans-membrane potential with slow responding probes is based on the molecular processes whereas a fast responding probes are based on the electronic phenomena [87, 132].

Operation of slow responding probes is based on their membrane binding and subsequent trans-membrane redistribution following a trans-membrane potential. Slow responding dyes, like other permeable ions, move across membranes until they reach electrochemical equilibrium. Their response time is counted in seconds or even minutes. Therefore, those probes are suitable for detecting changes in average membrane potentials of non-excitable cells caused by respiratory activity, ion channel permeability, drugs, to name a few. Their concentration gradient between both sides of the membrane obeys the Nernst equation [186, 187]:

$$\Delta\phi = RT \ln \frac{C_1}{C_2}, \tag{15}$$

Therefore, the accumulation of the dye on one side of the membrane reflects hyperpolarization, while its concentration decrease will reflect depolarization. The dye redistribution is visualized by fluorescence changes, which depend on its local concentration, i.e. self-quenching, or aggregation, to name a few.

Rhodamine-123 (R123), an example of the self-quenching dye, is the first dye to be used and remains one of the most popular in tracking mitochondrial membrane potential changes (Fig. 7) [188]. The advantage of using R123 as an indicator of membrane potential include its availability, high sensitivity (high quantum yield), specificity (against other environmental changes), non-invasiveness, and low interference with relevant metabolic

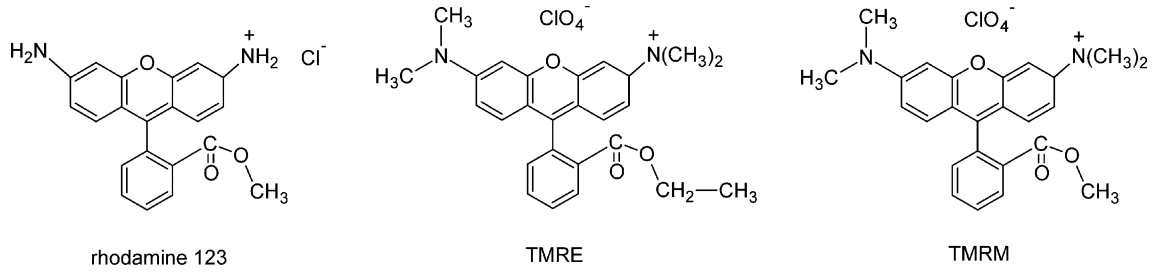

Fig. 7 Rhodamine dyes

processes. It was shown that the R123 fluorescence spectrum shifts to the red in response to mitochondrial energization. There is also empirical relationship between fluorescence intensity change and the membrane potential showing that the method may be qualitative [179]. The redistribution of R-123 in response to the membrane potential is followed by R-123 diminished fluorescence due to the self-quenching and spectral red shift. Therefore the two effects can be complementary applied in experimental protocols. In addition, the experiments can be carried out in the dynamic and static modes. The former is preferred if the availability of samples is not limited and if analysis of more than one factor on the same sample has to be assayed. The latter is preferred when the amount of samples is scarce and/or changes of the trans-membrane potential, induced by single effectors, are compared between different cell samples.

The relation between R123 fluorescence intensity, probe concentration and the trans-membrane potential has the following properties [189]:

1. The intensity of R123 fluorescence has the maximum at R123 concentration of 50 μM, and decreases to zero at higher concentrations due to the self-quenching.
2. The measured fluorescence intensity and the membrane potential are related by a non-linear calibration curve. The previously published and widely used empirical linear calibration curve is valid only over limited range of the potentials (approximately from 80 mV to 180 mV).
3. The shape of the calibration curve is sensitive to the details of the experimental protocol, including total concentration of the dye, the concentration of lipid in suspension, etc.
4. The predicted time course of the membrane potential changes in response to the perturbation (such as the addition of ADP to the respiration buffer) significantly differ from the observed transient in fluorescence intensity due to the slow response of R123 fluorescence (about 6 s).
5. Rhodamine is readily sequestered by cells or organelles and subsequently washed out of the cells once membrane potential is even transiently lost.
6. The rhodamine ester derivatives, tethraethyl-rhodamine ester, allow the cell loading with controlled amount of the dye available for mitochondria labeling [187].

Oxanols (Fig. 8) and selected cyanine dyes (Fig. 9) are another charged fluorescent dyes sensitive to the trans-membrane potential via redistribution across the membrane and accumulation on the membrane side with positive or negative potential built up, respectively [185, 190, 191]. The dye redistribution, similarly to rhodamine dyes, will follow the Nernst relation. (Eq. 15)

It has to be remembered that the local dye concentration can be biased by the membrane surface potential according to the Boltzman relation:

$$C_s = C_B \exp\left(\frac{-ze\Psi_S(z)}{kT}\right), \tag{16}$$

where the local charged dye concentration (C_S) depends both on the bulk concentration (C_B) and the local surface electrostatic potential, $\Psi_s(z)$.

The dye binding is accompanied by changes in its fluorescence properties. Oxonol V is often employed but it

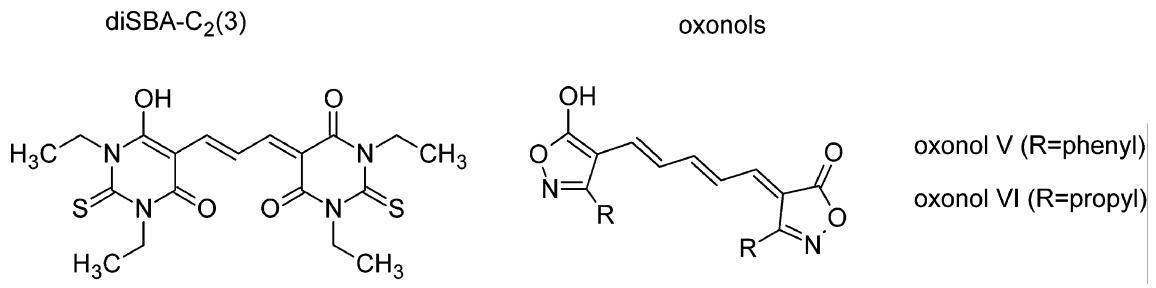

Fig. 8 Chemical structure of oxanol and its derivatives

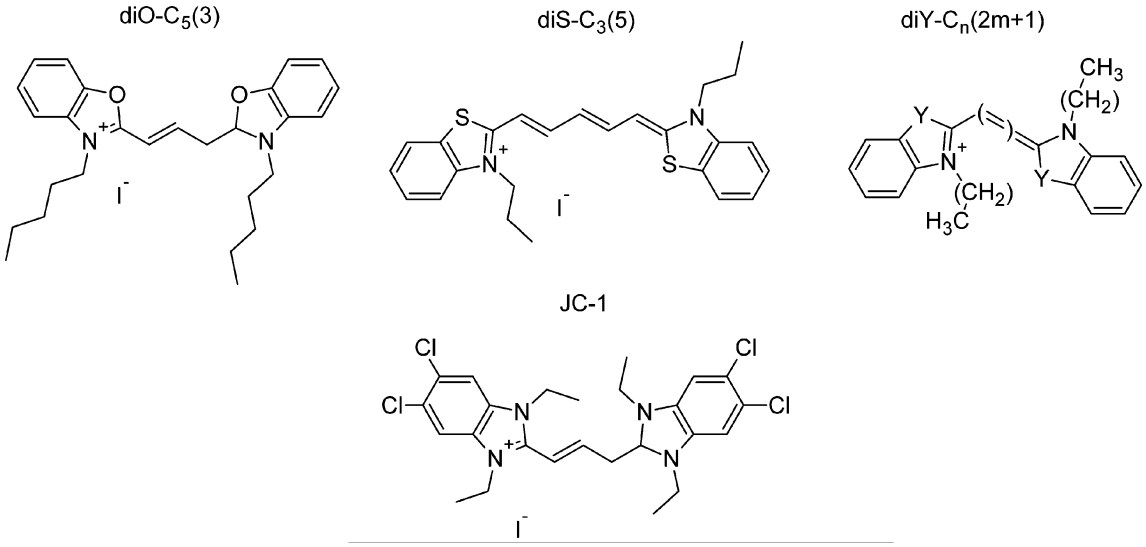

Fig. 9 Chemical structures of selected cationic cyanine dyes

exhibits pronounced fluorescence quenching at high concentrations. Intensity-independent methods are more convenient for quantitative measurements since they increase the accuracy of the results. The intensity-based methods are limited by variability in dye and/or vesicle concentrations or photobleaching. Oxonols upon binding to the membrane exhibit 20 nm shift of emission spectrum towards longer wavelengths. Tracking the emission spectrum position with a ratiometric approach can thus monitor the trans-membrane potential. Namely, fluorescence intensities are measured at two separate wavelengths, either at excitation or emission, corresponding to the fluorescence bands of free and bound dye. Then the ratio of intensities, related directly to the spectrum position, is calculated, [192–195].

In order to enhance the method sensitivity additional modifications were introduced. For example, an optical voltage sensor was proposed which consists of a membrane-bound fluorophore and an oxonol dye. The dye partitions into the membrane and distributes between the inner and the outer leaflet of the membrane as a function of the membrane potential. The two dyes are selected in such a way that the fluorescence resonance energy transfer is possible. The alteration in the local surface oxanol concentration results in changes of the energy transfer efficiency. In this system, fluorescence changes of up to 34% per 100 mV were achieved [196–198].

There is a serious intrinsic difficulty associated with the application of charged membrane permeable dyes; they increase the capacitive load on the membrane. Consequently, the charging of the membrane is seen as a slowing down of the rising trans-membrane potential and a decrease of the resting potential. The importance of this effect was demonstrated for excitable cells. During the onset of the membrane action potential, the current is facilitated, mainly, by the opening of the sodium channels (I_{Na}). Therefore, the change in membrane potential is approximately given by

$$\frac{dV}{dt} = \frac{I_{Na}}{C}, \tag{17}$$

and since I_{Na} remains approximately constant, an increase in C reduces $\frac{dV}{dt}$ so that the trans-membrane voltage develops more slowly. A further increase of the capacitive load results in complete abolition of the action potential.

Fast dyes, which monitor local electrostatic potential by adjusting their spacial valance electron arrangement in the fluorophore, reveal changes in the probe absorption and/or emission spectrum (electrochromism) [133, 199–202]. Those types of dyes are capable to monitor trans-membrane potential in the millisecond range. Examples of fast dyes are merocyanine 540, RH421, di-4-ANEPPS and di-8-ANEPPS. The spectral shift associated with a change in the membrane potential permits to develop a dual wavelength ratiometric approach [172, 201, 203]. It was shown that such dyes, as exemplified by the ANEP (aminonaphthethenyl-pyridinium), exhibit consistently responses in a variety of tissue, cell and model membrane systems [133, 172, 201, 203]. Initially, the dyes with the excitation spectrum sensitive to the local electric potential were developed [133, 199]. The ratio "R" is calculated from the part of the excitation spectrum where the total fluorescence is low and changes steeply with the wavelength. Using these fluorescence ratios the trans-membrane potential can be calibrated and measured.

When the relative changes in the membrane potential are measured both slow and fast fluorescent dyes can be used without additional data treatment. However, if the absolute

value of the potential is needed the appropriate calibration procedure is required. Specifically, the correlation of the fluorescent dye spectral properties needs to be calibrated against well-defined model system with predetermined membrane potential values. Ideally, the observed fluorescence changes at a given membrane potential, irrespective of its origin, should be reproducible and independent on the dye quantity [204]. The trans-membrane potential is usually generated in the lipid bilayer model systems by establishing a trans-membrane K^+ concentration difference in the presence of valinomycin resulting in the Nernst potential built up. For such system, the calculated $\Delta\Psi$ is correlated with the dye fluorescent intensities ratio (R) [14, 186, 205–208]. Certain caution is needed when using the procedure since the calculations of potential according to the Nernst equation might be incorrect (being underestimated due to the transient nature of the diffusion potentials). Moreover the signal changes induced by diffusion potentials may be influenced by the formation of lipid-soluble complexes between the ionophore (valinomycin), the permeant ion (K^+), and the probe. This calibration method was later modified to quantify $\Delta\Psi$ measurements in proteoliposomes with reconstituted H^+-ATPase from the plasma membrane of *S. pombe* [209].

Summary and perspectives

The HTS approaches are becoming widely used by pharmacological industry, in environmental studies and biological sciences. The selection of biologically relevant parameters and their subsequent evaluation using model systems is now a common strategy. Whereas, partition coefficient, solubility, membrane permeability and cellular toxicity are commonly evaluated the effect of active compounds on electrical properties of the biological systems are seldom used in large-scale studies. The enormous advancement of fluorescence techniques enabled development of the new membrane electrostatic potential tests and their HTS application. The electrical properties of membranes can be now efficiently and reliably measured and/or visualized. The first trans-membrane potential determination was performed on mitochondria using cationic rhodamine 123 [188]. The methyl and ethyl esters of tetramethylrhodamine (TMRM and TMRE) are currently the preferred dyes for the determination of membrane potential in cells by quantitative imaging [20, 170, 187]. They are membrane permeable and their strong fluorescence implies their application at low concentrations, thus avoiding the aggregation and the local alterations in the membrane potential. As their fluorescence is relatively insensitive to the environment, spatially resolved fluorescence of TMRM and TMRE presents an unbiased profile of their trans-membrane distribution that can be related directly to the membrane potential via the Nernst equation [20]. There are now commercially available products designed for electric activity evaluation in living cells (Axiom Biotechnologies Inc, USA). In this assay the resonance energy transfer between two dyes is used as indication of the modulation of the cell membrane potential. A number of other applications as well as further improvements of this technique are outlined in UK patent no. UKPA. 9406464.9. Fluorescence methods are now combined with electrophysiological tool-kids providing comprehensive excitable system characterization [89, 210]. It is possible now to detect a broad range of cellular effects using dedicated fluorescent probes including for example; changes in the mitochondrial and cytoplasmic membrane potentials occurring in the early stages of receptor-mediated activation processes [211, 212], membrane potential-related changes indicating bacterial injury [213], shear stress effects in endothelial cells [214] or studies on mitochondrial functionality during apoptosis [215]. The combination of fluorescence, molecular biology methods, and genetic engineering allows designing cellular models, which enable single molecule studies on membrane channels [85, 86, 171, 216] or to combine them with independently measured intracellular parameters [217–219]. Genetically encoded probes are now used for membrane potential determination [220, 221] or even to study neural network systems [222]. Site-specific fluorescence measurements of ion channels under voltage-controlled conditions allowed direct tracking of the conformational change of the voltage sensor in expression systems ranging from oocytes [223–226] to various cells [173, 227, 228]. By introducing cysteine residues in the specified locations of the channel protein, it is possible to attach fluorescent dyes at predetermined sites and thus report local changes in the electrical field strength and correlate it with channel functioning [229, 230]. The variety of new optical methods emerges for studies of membrane potential using spectroscopy, microscopic image analysis [231–234], non-linear optical measurements [235, 236] or second-harmonic generation microscopy action potential recording [88, 237, 238]. The combination of improved experimental data acquisition and handling, combined with molecular dynamic simulations, introduces new quality to understanding and subsequent applications of knowledge on electrical properties of biological systems [132].

All those developments allow for the rational design of a comprehensive fluorescence platform, based on model supramolecular aggregates, model membranes or even whole cells, for the characterization of biological systems [239–244]. Moreover, the miniaturization and the application of automated routines will make the massive scale measurements of membrane potentials possible [245–248].

Acknowledgements This work was possible thanks to the financial support from Polish Ministry of Science and Higher Education (Grant #N N518 1903 33) and from the Centre of Biomedical Engineering, Wrocław University of Technology.

References

1. Blunck R, Chanda B, Bezanilla F (2005) Nano to micro—fluorescence measurements of electric fields in molecular and fenetically specified neurons. J Membrane Biol 208:91–102
2. Honig BM, Hubbell WL, Flewelling RF (1986) Electrostatic interactions in membranes and proteins. Ann Rev Biophys Biophys Chem 15:163–193
3. Cevc G (1990) Membrane electrostatics. Biochim Biophys Acta 1031–1033
4. Langner M, Cafiso SD, Marcelja S, McLauglin S (1990) The electrostatic properties of the phosphoinositides: theoretical and experimental results obtained with memrane contaning either PI, a monovalent lipid, or PIP2, a trivalent lipid. Biophys J 57:335–349
5. McLaughlin S (1989) The eletrostatic properties of membranes. Annu Rev Biophys Biophys Chem 18:113–136
6. Spitzer JJ, Poolman B (2005) Electrochemical structure of the crowded cytoplasm. Trends Biochem Sci 30:536–541
7. Collins KD (1995) Sticky ions in biological systems. Proc Natl Acad Sci USA 92:5553–5557
8. Collins KD (1997) Charge density-dependent strenght of hydration and biological structure. Biophys J 72:65–76
9. Ball P (2008) Water as an active constituent in cell biology. Chem Rev 108:74–108
10. Swartz KJ (2008) Sensing voltage across lipid membranes. Nature 456:891–897
11. Schmidt D, Jiang QX, MacKinnon R (2006) Phospholipids and the origin of cationic gating charges in voltage sensors. Nature 444:775–779
12. Paolo GD, Camilli PD (2006) Phosphoinositides in cell regulation and membrane dynamics. Nature 443:651–657
13. McLaughlin S, Murray D (2005) Plasma membrane phosphinositide organiztion by protein electrostatics. Nature 438:605–611
14. Sten-Knudsen O (2002) Biological membranes: theory of transport potentials, and electric impulses. Cambridge University Press, Cambridge
15. Langner M, Kubica K (1999) The electrostatics of lipid surfaces. Chem Phys Lipids 101:3–35
16. Cevc G (1993) Electrostatic characterization of liposomes. Chem Phys lipids 64:163–186
17. Brockman H (1994) Dipole potential of lipid membranes. Chem Phys Lipids 73:57–79
18. Petersen PB, Saykally RJ (2006) On the nature of ions at the liquid water surface. Ann Rev Phys Chem 57:333–364
19. Olivotto M, Arcangeli A, Carla M, Wanke E (1996) Electric fields at the plasma membrane level: a neglected element in the mechanisms of cell signalling. BioEssays 18:495–503
20. Loew LM (1993) The electrical properties of membranes. Biomembranes Physical aspects 341–371
21. Hille B (1992) Ionic channels of excitable membranes. Sinauer Associates Inc, Sunderland
22. Galluzzi L, Zamzami N, de-La-Motte-Rouge T, Lemair C, Brenner C, Kroemer G (2007) Methods for the assessment of mitochondrial membrane permeabilization in apoptosis. Apoptosis 12:803–813
23. Ehringer WD, Su S, Chiang B, Stillwell W, Chien S (2002) Destabilizing effects of fructose-1, 6-bisphophate on membrane bilayers. Lipids 37:885–892
24. Luzardo M, Peltzer G, Disalvo EA (1998) Surface potential of lipid interfaces formed by mixturs of phosphatidylcholine of different chain lengths. Langmuir 14:5858–5862
25. Dani JA (1986) Ion-channel entrance influence permeation. Net charge, size, shape and binding considerations. Biophys J 49:607–618
26. Jordan P (1987) How pore mouth charge distributions alter the permeability of transmembrane ionic channels. Biophys J 51:297–311
27. Kell MJ, DeFelice LJ (1988) Surface charge near the cardiac inward rectifier channel measured from single channel conductance. J Membrane Biol 102:1–10
28. Moczydlowski E, Alvaraz O, Vergara C, Latorre R (1985) Effects of phospholipid surface charge on the conduction and gating of a Ca^{+2} activated K^{+} channel in planar lipid bilayers. J Membrane Biol 83:273–282
29. Pertou S, Ordway RW, Hamilton JA, Walsh-Jr JV, Singer JJ (1994) Structural requirements for charged lipid molecules to directly increase or supress K1 channel activity in smooth muscle cells. J Gen Physiol 103:471–486
30. Gilson MK, Honig BH (1988) Energetics of charge-charge interctions in proteins. Proteins 3:32–52
31. Huang JK, Warshel A (1988) Why ion pair reversal by protein engineering is unlikely to succed. Nature 334:270–272
32. Matos PM, Goncalves S, Santos NC (2008) Interaction of peptides with biomembranes assessed by potential-sensitive fluorescent probes. J Pept Sci 14:407–415
33. Wall JS, Golding S, van-Veen M, O'Shea PS (1995) The use of flurescein-phosphatidylethanolamine as a real-time probe for peptide-membrane interaction. Mol Membr Biol 12:183–192
34. Silvestroni L, Fiorini R, Palleschi S (1997) Pertitioning of the orgnochlorine insecticide lindane into humn sperm surface induces membrane depolarization and Ca+2 influx. Biochem J 321:691–698
35. Scherer PG, Seelig J (1989) Electric charge efects on phospholipid headgroups: phosphatidylcholine in mixtures with cationic and anionic amphiphiles. Biochemistry 28:7720–7728
36. Jurkiewicz P, Sykora J, Olzynska A, Humpolickova J, Hof M (2005) Solvent relaxation in phospholipid bilayers: principles and recent applications. J Fluorescence 15:883–892
37. Bangham AD, Mason W (1979) The effect of some general anesthetics on the surface potential of lipid monolayers. Br. J, Pharmacol, 66
38. Gabev E, Kasianowicz J, Abbot T, McLaughlin S (1989) Binding of neomycin to phosphatidylinositl 4, 5-bisphosphate (PIP2). Biochim Biophys Acta 979:105–112
39. Haydon DA, Elliot JR (1986) Surface potential changes in lipid monolayers and the "cut-off" in anesthetic effects on N-alkanols. Biochim Biophys Acta 863:337–340
40. Clarke RJ, Lupfert C (1999) Influence of anions and cations on the dipole potential of phosphatidylcholine vesicles: a basis for the Hofmeister effect. Biophys J 76:2614–2624
41. Clarke RJ, Kane DJ (1997) Effect of lipid structure on the dipole potential of phopshatidylcholine bilayers. Biochim Biophys Acta 1327:269–278
42. Diaz S, Amalfa F, Biondi-de-Lopez AC, DiSalvo EA (1999) Effect of water polarized at the carbonyl groups of phsophatidylcholines on the dipole potential of lipid bilayers. Langmuir 15:5170–5182
43. Gawrisch K, Ruston D, Zimmerberg J, Persegian VA, Rand RP, Fuller N (1992) Membrane dipole potentials, hydration forces, and the ordering of water at membrane surface. Biophys J 61:1213–1223
44. Peterson U, Mannock DA, Lewis RNAH, Pohl P, McElhaney RN, Pohl EE (2002) Orgin of membrane dipole potential: contribution of the phospholipid fatty acid chains. Chem Phys Lipids 117:19–27

45. Shinoda W, Shimizu M, Okazaki S (1998) Molecular dynamic study on electrostatic properties of a lipid bilayer: polarization, electrostatic potential, and the effects on structure and dynamics of water near the interface. J Phys Chem B 102:6647–6654
46. Marrink SJ, Tieleman DP, vanBuuren AR, Berendsen HJC (1996) Membranes and water: an interesting relationship. Faraday DIscuss 103:191–201
47. Zheng C, Vanderkooi G (1992) Molecular origin of the internal dipole potential in lipid bilayers: calcultion of the electrostatic potential. Biophys J 63:935–941
48. Gross E, Bedlack RS, Loew LM (1994) Dual-wavelength ratiometric fluorescence measurements of the membrane dipole potential. Biophys J 67:208–216
49. Seelig J, Macdonald PM, Scherer PG (1987) Phospholipid head goup as sensors of electric charge in membranes. Biochemistry 26:7535–7541
50. Cafiso DS (1998) Dipole potentials and spontaneous curvature: membrane properties that could medaite anesthesia. Toxicol Lett 101:431–439
51. Alakoskela JMI, Soderlund T, Holopainen JM, Kinnunen PKJ (2004) Dipole potential and head-group spacing are determinants for the membrane partitioning of pregnanolone. Mol Pharmacol 66:161–168
52. Hogberg CJ, Lyubartsev AP (2008) Effect of local anesthetic lidocaine on electrostatic properties of a lipid bilayer. Biophys J 94:525–531
53. Schamberger J, Clarke RJ (2002) Hydrophobic ion hydration and the magnitude of the dipole potential. Biophys J 82:3081–3088
54. Anderson OS, Finkelstein A, Katz I, Cass A (1976) Effect of phloretin on the permeability of thin lipid membranes. J Gen Physiol 67:749–771
55. Cafiso DS (1995) Influence of charges and dipoles on macromolecular adsorption and permeability. In: Disalvo EA, Simon SA (eds) Permeability and stability of lipid bilayers. CRC Press, Boca Raton
56. Hladky SB, Haydon DA (1973) Membrane conductance and surface potential. Biochim Biophys Acta 318:464–468
57. Flewelling RF, Hubbell WL (1986) The membrane dipole potential in a total membrane potential model. Applications to hydrophobic ion interactions with membranes. Biophys J 49:541–552
58. Franklin JC, Cafiso DS, Flewelling RF, Hubbell WL (1993) Probes of membrane electrostatics: synthesis and voltge-dependent partitioning of negative hydrophobic ion spin labeles in lipid vesicles. Biophys J 64:642–653
59. Phillips LR, Cole CD, Hendershot RJ, Cotton M, Cross TA, Busath DD (1999) Noncontact dipole effects on channel permeation. III. Anomalous proton conductance effects in gramicidin. Biophys J 77:2492–2501
60. Duffin RL, Garrett MP, Flake KB, Durrant JD, Busath DD (2003) Modulation of lipid bilayer interfacial dipole potential by phloretin, RH421, and 6-ketocholesterol as probed by gramicidin channel conductance. Langmuir 19:1439–1442
61. Cladera J, O'Shea P (1998) Intramembrane molecular dipoles affect the membrane insertion and folding of a model amphiphilic peptide. Biophys J 74:2434–2442
62. Cladera J, O'Shea P, Hadgraft J, Valenta C (2003) Influence of molecular dipoles on human skin permeability: use of 6-ketocholesterol to enhance transdermal delivery of bacitracin. J. Pharm, Sci, 92
63. Maggio B (1999) Modulation of phospholipase A2 by electrostatic fields and dipole potential of glycosphingolipids in monolayers. J Lipid Res 40:930–939
64. Alakoskela JMI, Kinnunen PKJ (2001) Control of a redox reaction on lipid bilayer surface by membrane dipole potential. Biophys J 80:294–304
65. Reyes J, Benos DJ (1984) Changes in interfacial potentials induced by carbonylcyanide phenylhydrazone uncouplers: possible role in inhibition of mitochondrial oxygen consumption and other transport processes. Membr Biochem 5:243–268
66. Starkov AA, Bloch DA, Chernyak BV, Dedukhova VI, Mansurova SE, Severina II, Simonyan RA, Vygodina TV, Skulchev VP (1997) 6-ketocholesterol is recoupler fo mitochondria, chromatophores and cytochrome oxidase proteoliposomes. Biochim Biophys Acta 1318:159–172
67. Starke-Petrovic T, Turner N, Else PL, Clarke RJ (2005) Electric field strength of membrane lipids from vertebrate species: membrane lipid composition and Na1, K1-ATPase molecular activity. Am J Physiol Regul Integr Comp Physiol 288:R663–R670
68. Cladera J, Martin I, Ruysschaert JM, O'Shea P (1999) Characterization of the sequence of interactions of the fusion domain of the simian immunodeficiency virus with membranes. J Biol Chem 274:29951–29959
69. Asawakarn T, Cladera J, O'shea P (2001) Effects of the membrane dipole potential on the interaction of saquinavir with phospholipid membranes and plasm membrane receptor of caco-2 cells. J Biol Chem 276:38457–38463
70. Luker GD, Flagg TP, Sha Q, Luker KE, Pica CM, Nichols CG, Piwnica-Worms D (2001) MDR1 P-glycoprotein reduces influx of substrates without affecting membrane potential. J Biol Chem 276:49053–49060
71. Simon SA, McIntosh TJ (1989) Magnitude of the solvation pressure depends on dipole potential. Proc Natl Acad Sci USA 86:9263–9267
72. Simon SA, McIntosh TJ, Magid AD, Needham D (1992) Modulation of the interbilayer hydration pressure by the addition of dipols at the hydrocarbon/water interface. Biophys J 61:786–799
73. Gennis RB (1989) Biomembranes. Molecular structure and functions, Springer-Verlag, New York
74. Alper J (2002) Breaching the membrane. Science 296:838–839
75. Castle NA (2005) Aquaporins as targets for drug discovery. DDT 10:485–493
76. Li X, Chan WK (1999) Transport, metabolism and elimination mechanisms of anti-HIV agents. Adv Drug Deliv Rev 39:81–103
77. Nava-Ocampo AA, Bello-Ramirez AM (2004) Lipophilicity affects the pharmacokinetics and toxicity of local anaesthetic agents administered by caudal block. Clin Exp Pharmacol Physiol 31:116–118
78. White RE (2000) High-throughput screening in drug metabolism and pharmacokinetic support of drug discovery. Annu Rev Pharmacol Toxicol 40:133–157
79. Agoram BM, Martin SW, van-der-Graaf PH (2007) The role of mechanism-based pharmacokinetic-pharmacodynamic (PK-PD) modelling in translational research of biologics. Drug Disc Today 12:1018–1024
80. von-Kleist M, Huisinga W (2007) Physiologically based pharmacokinetic modelling: a sub-compartmentalized model of tissue distribution. J Pharmacokinet Pharmacodyn 34:789–806
81. Mager DE (2006) Quantitative structure-pharmacokinetic/pharmacodynamic relationship/. Adv Drug Deliv Rev 58:1326–1356
82. Watt AP, Morrison D, Evans DC (2000) Approaches to higher-throughput pharmacokinetics (HTPK) in drug discovery. DDT 5:17–24
83. Clark DE (2003) In silico prediction of blood-brain barrier permeation. DDT 8:927–933
84. Wells JA, McClendon CL (2007) Reaching for high-hanging fruit in drug discovery at protein-protein interfaces. Nature 450:1001–1009
85. Ataka K, Pieribone VA (2002) A genetically targetable fluorescent probe of channel gating with rapid kinetics. Biophys J 82:509–516

86. Chudakov DM, Lukyanov S, Lukyanov KA (2005) Fluorescent proteins as a toolkit for in vivo imaging. Trends Biotech 23:605–613
87. Cohen LB, Salzberg BM (1978) Optical measurements of membrane potential. Rev Physiol Biochem Pharmacol 83:35–88
88. Dombeck DA, Blanchard-Desce M, Webb WW (2004) Optical recording of action potentials with second-harmonic generation microscopy. J Neurosci 24:999–1003
89. Duclohier H (2000) Coupling of simultaneous fluorescence and electrophysiology: historical survey, contributions, and prospects. J Fluorescence 10:127–134
90. Valeur B (2001) Molecular fluorescence: principles and applications. Wiley-VCH Verlag GmbH, Weinheim
91. Angel I, Bar A, Haring R (2002) Bioactive lipids and their receptors. Curr Opin Drug Discov Develop 5:78–740
92. Bandhuvula P, Saba JD (2007) Sphingosine-1-phosphate lyase in immunity and cancer: silencing the siren. Trends Mol Med 13:210–217
93. Chen CS, Petterson MC, Wheatley CL, O'Brien JF, Pagano RE (1999) Broad screening test for sphingolipid-storage diseases. Lancet 354:901–905
94. Hannun YA (1997) Apoptosis and the dilemma of cancer chemotherapy. Blood 89:1845–1853
95. Kozubek A, Tyman JHP (1999) Resorcinolic lipids, the natural non-isoprenoid phenolic amphiphiles and their biological activity. Chem Rev 99:1–25
96. Levade T, Auge N, Veldman RJ, Cuvillier O, Negre-Salvayre A, Salvayre R (2001) Sphibgolipid mediators in cardiovascular cell biology and pathology. Circ Res 89:957–968
97. Listenberger LL, Ory DS, Schaffer JE (2001) Palmitate-induced apoptosis can occur through a ceramide-independent pathway. J Biol Chem 276:14890–14895
98. Mannori G, Barletta E, Mugnai G, Ruggieri S (2000) Interaction of tumor cells with vascular endothelia: role of platelet-activating factor. Clin Exp Metastasis 18:89–96
99. Merrill AH, Schmelz EM, Dillehay DL, Spiegel S, Shayman JA, Schroeder JJ, Riley RT, Voss KA, Wang E (1997) Sphingolipids—The enigmatic lipid class: biochemistry, physiology, and pathophysiology. Toxicol App Pharmacol 142:208–225
100. Ogretmen B, Hannun YA (2004) Biologically active sphingolipids in cancer pathogenesis and treatment. Nat Rev 4:604–616
101. Pagano RE, Puri V, Dominguez M, Marks DL (2000) Membrane traffic in sphingolipid storage diseases. Traffic 1:807–815
102. Siess W, Essler M, Brandl R (2000) Lysophospatidic acid and sphingosine 1-phosphate: two lipid villains provoking cardiovascular diseases? IUBMB Life 49:167–171
103. Subbaiah PV, Sargis RM (2001) Sphingomyelin: a natural modulator of membrane homeostasis and inflammation. Med Hypothesis 57:135–138
104. Tamama K, Okajima F (2002) Sphingosine 1-phosphate signaling in atherosclerosis and vascular biology. Curr Opin Lipidol 13:489–495
105. van-Meer G (2005) Cellular lipidomics. EMBO J 24:3159–3165
106. Nagle JF, Tristram-Nagle S (2000) Structure of lipid bilayers. Biochim Biophys Acta 1469:159–195
107. Mouritsen OG, Jorgensen K (1998) A new look at lipid-membrane structure in relation to drug research. Pharm Res 15:1508–1519
108. Jones MN, Chapman D (1995) Micelles, monolayers and biomembranes. Wiley, New York
109. Lakowicz JR (1999) Principles of fluorescence spectroscopy. Kluwer Academic/Plenum Publishers, New York
110. Gratton E, Barry NP, Beretta S, Celli A (2001) Multiphoton fluorescence microscopy. Methods 00:103–110
111. Fitch RW, Xiao Y, Kellar KJ, Daly JW (2003) Membrane potential fluorescence: a rapid and highly sensitive assay for nicotinic receptor channel function. PNAS 100:4909–4914
112. Eisenberg M, Gresalfi T, Riccio T, McLaughlin S (1979) Adsorption of monovaent cations to bilayer membranes containing negative phospholipids. Biochemistry 18:5213–5223
113. Kubica K, Langner M, Gabrielska J (2003) The dependence of fluorescein -PE fluorescence intensity on lipid bilayer state. Evaluating the interaction between the probes and lipid molecules. Cell Mol Biol Lett 8:943–954
114. Geddes CD (2001) Optical halide sensing using fluorescence quenching: theory, simulations and applications—a review. Meas Sci Technol 12:R53–R88
115. Winiski M, Eisenberg M, Langner M, McLaughlin S (1988) Fluorescence probes of electrostatic potential 1 nm from the membrane surface. Biochemistry 27:386–392
116. Chattopadhyay A (1990) Chemistry and biology of N-(7-nitrobenz-2-oxa-1, 3-diazol-4-yl)-labeled lipids: fluorescent probes of biological and model membranes. Chem Phys Lipids 53:1–15
117. Chattopadhyay A, London E (1987) Parallax method for direct measurement of membrane penetration depth utilizing fluorescence quenching by spin-labeled phospholipids. Biochemistry 26:39–45
118. Blatt E, Sawyer WH (1985) Depth-dependent flourescent quenching in micelles and membranes. Biochim Biophys Acta 822:43–62
119. Langner M, Winiski A, Eisenberg M, McLaughlin A, McLaughlin S (1988) The electrostatic potential adjacent to bilayer membranes containing either charged phospholipids or gangliosides. New Trends Gangloside Res 14:121–130
120. McLaughlin S, Langner M, McDaniel R (1989) Experimental tets of the Gouy-Chapman theory using phospholipid bilyers. Electrochimica Acta 34:1903–1904
121. Kraayenhof R, Sterk GJ, Sang HWWF (1993) Probing biomembrane interfacial potential and pH profiles with a new type of float-like fluorophores positioned at varying distance from the membrane surface. Biochemistry 32:10057–10066
122. Epand RM, Kraayenhof R (1999) Fluorescent probes used to monitor membrane interfacial polarity. Chem Phys Lipids 101:57–64
123. Kraayenhof R, Sterk GJ, Sang HWWF, Krab K, Epand RM (1996) Monovalent cations differentially affect membrane surface properties and membrane curvature, as revealed by fluorescent probes and dynamic light scattering. Biochim Biophys Acta 1282:293–302
124. Fromherz P, Masters M (1974) Interfacial pH at electrically charged lipid monolayers investigated by the lipoid pH-indicator method. Biochim Biophys Acta 356:270–275
125. Matsumoto H, Koyama Y, Tanioka A (2003) Interaction of proteins with weak amphoteric charged membrane surface: effect of pH. J Coll Interface Sci 264:82–88
126. Langner M, Gabrielska J, Kleszczynska H, Pruchnik H (1998) Effect of phenyltin compounds on lipid bilayer organization. Appl Organometallic Chem 12:99–107
127. Langner M, Gabrielska J, Przestalski S (2000) Adsorption of phenyl compounds onto phosphatidylcholine/cholesterol bilayers. Appl Organometallic Chem 14:25–33
128. Kalinin SV, Molotkovsky JG (2000) Anion binding to lipid bilayers: determination using fluorescent membrane probe by direct quenching or by competitive displacement approaches. J Biochem Biophys Meth 46:39–51
129. Olzynska A, PRzybylo M, Gabrielska J, Trela Z, PRzestalski S, Langner M (2005) Di- and tri-phenyltin chlorides transfer across a model lipid bilayer. App. Organometall, Chem, 19
130. Przybylo M, Olżyńska A, Han S, Ożuhar A, Langner M (2007) A fluorescence method for determination transport of charged cmpounds across lipid bilayer. Biophys Chem 129:120–125
131. Przybylo M, Borowik T, Langner M (2007) Application of liposome based sensors in high-throughput screening systems. Combinatorial Chem HTS 10:441–450

132. Demchenko AP, Yesylevskyy SO (2009) Nanoscopic description of biomembrane electrostatics: results of molecular dynaic simulations and fluorescence probing. Chem Phys Lipids 160:63–84
133. Fluhler E, Burnham VG, Loew LM (1985) Spectra, membrane binding and potentiometric responses of new charge shift probes. Biochemistry 24:5749–5755
134. Kuhn B, Fromherz P, Denk W (2004) HIgh sensitivity of Stark shift voltage-sensing dyes by one- or two photon excitation near the red spectral edge. Biophys J 87:631–639
135. Malkov DY, Sokolov VS (1996) Fluorescent styryl dyes of the RH series affect a potential drop on the membrane/solution boundary. Biochim Biophys Acta 1278:197–204
136. Mukherjee S, Chattopadhyay A, Samnta A, Soujnya T (1994) Dipole moment change of NBD group upon excitation studied using solvatochromic and quantum chemical approaches: implications in membrane reseach. J Phys Chem 98:2809–2812
137. Ohta N, Ito T, Okazaki S, Yamazaki I (1997) External electric field effects on absorption and fluorecence spectra of monomer and dimer of oxacarbocyanine in Langmuir-Blodgett films. J Phys Chem B 101:10213–10220
138. Brown DA, London E (1998) Structure and origin of ordered lipid domains in biological membranes. J Membrane Biol 164:103–114
139. Brown DA, London E (1998) Functions of lipid rafts in biological membranes. Annu Rev Cell Dev Biol 14:111–136
140. Edidin M (1990) Molecular associations and lipid domains. Curr Top Membr Transp 36:81–96
141. Edidin M (2001) Shrinking patches and slippery rafts: scales of domains in the plasma membrane. Trends cell BIol 11:492–496
142. Engelman DM (2005) Membranes are more mosaic than fluid. Nature 438:578–580
143. Korlach J, Baumgart T, Webb WW, Feigenson GW (2005) Detection of motional heterogeneities in lipid bilayer membranes by dual probe fluorescence correlation spectroscopy. Biochim Biophys Acta 1668:158–163
144. Shaikh SR, Edidin MA (2006) Membranes are not just rafts. Chem Phys Lipids 144:1–3
145. Bevers EM, Comfurius P, Dekkers DWC, Harmsma M, Zwall RFA (1998) Transmembrane phospholipid distribution in blood cells: control mechanisms and pathophysiological significance. Biol Chem 379:973–986
146. Bevers EM, Comfurius P, Dekkers DWC, Zwall RFA (1999) Lipid translocation across the plasma membrane of mammalian cells. Biochim Biophys Acta 1439:317–330
147. Daleke DL (2003) Regulation of transbilayer plasma membrane phospholipid asymmetry. J Lipid Res 44:233–242
148. Connor J, Pak CC, Schroit AJ (1994) Exposure of phosphatidylserine in the outer leaflet of human red blood cells: relationship to cell density, cell age, and clearance by monomolecular cells. J Biol Chem 269:2399–2406
149. Fadok VA, Voelker DR, Campbell PA, Cohen JJ, Bratton DL, Henson PM (1992) Exposure of phosphatidylserine on the surface of apoptotic lymphocytes triggers specific recognition and removal by macrophages. J Immunol 148:2207–2211
150. Ishaque A, Al-Rubeai M (1998) Use of intracellular pH and annexin-V flow cytometric assays to monitor apoptosis and its supression by bcl-2 over-expression in hybrydoma cell culture. J Immunol Methods 221:43–57
151. Plasier B, Lloyd DR, Paul GC, Thomas CR, Al-Rubeai M (1999) Automatic imge analysis for quantification of apoptosis in animal cell culture by annexin-V affinity assay. J Immunol Methods 229:81–95
152. Franklin JC, Cafiso DS (1993) Internal electrostatic potentials in bilayers: measuring and controlling dipole potentials in lipid vesicles. Biophys J 65:289–299
153. Clarke RJ (2001) The dipole potential of phospholipid membranes and methods for its detection. Adv Coll Interface Sci 89–90:263–281
154. Klymchenko AS, Duportail G, Mely Y, Demchenko AP (2003) Ultrasensitive two-color fluorescence probes for edipole potential in phospholipid membranes. PNAS 100:11219–11224
155. M'Baye G, Shynkar VV, Klymchenko AS, Mely Y, Duportail G (2006) Membrane dipole potential as measured by ratiometric 3-hydoxyflavone fluorescence probes: accounting for hydration effects. J Fluorescence 16:35–42
156. Zouni A, Clarke RJ, Holzwarth JF (1994) Kinetics of solubilization of styryl dye aggregates by lipid vesicles. J Phys Chem 98:1732–1738
157. Clarke RJ, Kane DJ (1997) Optical detection of membrane dipole potential: avoidance of fluidity and dye-induced effects. Biochim Biophys Acta 1323:223–239
158. Lewis RNAH, McElhaney RN (2000) Surface charge markedly attenuates the nonlamellar phase-forming propensities of lipid bilayer membranes: calorimetric and ^{31}P-nuclear magnetic resonance studies of mixtures of cationic, anionic, and zwitterionic lipids. Biophys J 79:1455–1464
159. Li SJ, Yamashita Y, Yamazaki M (2001) Effect of electrostatic interactions on phase stability of cubic phases of membranes of monoolein/dioleoylphosphatidic acid mixtures. Biophys J 81:983–993
160. Tarahovsky YS, Arsenault AL, MacDonald RC, McIntosh TJ, Epand RM (2000) Electrostatic control of phospholipid polymorphism. Biophys J 79:3193–3200
161. Loew LM (1988) Spectroscopic membrane probes. CRC Press, Boca Raton
162. Gowen JA, Markham JC, Morrison SE, Cross TA, Busath DD, Mapes E, Schumaker MF (2002) The role of Try side chains in tuning single proton conduction through gramicidin channels. Biophys J 83:880–898
163. Neher E, Eibl HJ (1977) The influence of phospholipid polar groups on gramicidin A channels. Biochim Biophys Acta 464:37–44
164. Shapovalov VL, Kotova EA, Rokitskaya TI, Antonenko YN (1999) Effect of Gramicidin A on the dipole potential of phospholipid membranes. Biophys J 77:299–305
165. Rokitskaya TI, Antonenko YN, Kotova EA (1997) Effect of the dipole potential of a bilayer lipid membrane on gramicidin chnnel disociation kinetics. Biophys J 73:850–854
166. Cseh R, Benz R (1999) Interaction of phloretin with lipid monolayers: relationship between structural chnges and dipole potential change. Biophys J 77:1477–1488
167. Amanullah A, Hewitt CJ, Nienow AW, Lee C, Chartrain M, Buckland BC, Drew SW, Woodley JM (2002) Application of multi-parameter flow cytometry using fluorescence probes to study substrate toxicity in the indene bioconversion. Biotechnol Bioeng 80:239–249
168. Bezrukov SM (2000) Ion channels as molecular Couter counters to probe metabolite transport. J Memebrane Biol 174:1–13
169. Rieseberg M, Kasper C, Reardon KF, Scheper T (2001) Flow cytometry in biotechnology. Appl Microbiol Biotechnol 56:350–360
170. Gross D, Loew LM (1989) Fluorescence indicators of membrane potential: microspectrofluorometry and imaging. In: Wang Y, Taylor DL (eds) Methods in Cell Biology. Academic, New York, p 30
171. Guerrero G, Isacoff EY (2001) Genetically encoded optical sensors of neuronal activity and cellular function. Curr Opin Neurobiol 11:601–607
172. Bedlack RS, Wei MD, Loew LM (1992) Localized membrane depolrizations and localized intracellular calcium influx during electric field-guided neurite growth. Neuron 9:393–403

173. Bluck R, Starace DM, Correa AM, Benzanilla F (2004) Detecting rearrangements of shaker and NaChBac in rel-time with fluorescence spectroscopy in patch-clamped mammalian cells. Biophys J 86:3966–3980
174. Canepari M, Vogt K, Zecevic D (2008) Combining voltage and calcium imaging from neuronal dendrites. Cell Mol Neurobiol 28:1079–1093
175. Chanda B, Blunck R, Faria LC, Schweizer FE, Mody I, Bezanilla F (2005) A hybrid approach to measuring electrical activity in gentically specified neurons. Nat Neurosci 8:1619–1626
176. Kasza KE, Rowat AC, Liu J, Angelini TE, Brangwynne CP, Koenderink GH, Koenderink GH, Weitz DA (2007) The cell as a material. Curr Opin Cell Biol 19:101–107
177. Leopoldo M, Lacivita E, Berardi F, Perrone R (2009) Developments in fluorescence probes for receptor research. Drug Disc Today 14:706–712
178. Hüser J, Lipp P, Neggli E (1996) Confocal microscopic detection of potential-sensitive dyes used to reveal loss of voltage control during patch-clamp experiments. Eur J Physiol 433:194–199
179. Emaus RKR, Grunwald JJ, Lemasters JJ (1986) Rhodamine 123 as a probe of transmembrane potential in isolated rat-liver mitochondria: spectral and metabolic properties. Biochim Biophys Acta 850:436–448
180. Baracca A, Sgarbi G, Solaini G, Lenaz G (2003) Rhodamine 123 as a probe of mitochondrial membrane potential: evaluation of proton flux through F0 during ATP synthesis. Biochim Biophys Acta 1606:137–146
181. Nicholls DG (2006) Simultaneous monitoring of ionophore- and inhibitor-mediated plasma and mitochondrial membrane potential changes in culture neurons. J Biol Chem 281:14864–14874
182. Rottenberg H, Wu S (1998) Quantitative assay by flow cytometry of the mitochondrial membrnae potential in intact cells. Biochim Biophys Acta 404:393–404
183. Reers M, Smith TW, Chen LB (1991) J-aggregate formation of a carbocyanine as a quantitative fluorescent indicator of membrane potential. Biochemistry 30:4480–4486
184. Kalenak A, McKenzie RJ, Conover TE (1991) Response of the electrochromic dye, merocyanine 540, to membrane potential in rat liver mitochondri. J Membr Biol 123:23–31
185. Cooper CE, Bruce D, Nicholls P (1990) Use of oxonol V as probe of membrane potential in proteoliposomes containing cytochrome oxidase in the submitochondrial orientation. Biochemistry 29:3859–3865
186. Plasek J, Sigler K (1996) Slow fluorescent indicators of membrane potential: a survay of different approaches to probe response analysis. J Photochem Photobiol B 33:101–124
187. Ehrenberg B, Montana V, Wei MD, Wuskall JP, Loew LM (1988) Membrane potential can be determined in individul cells from the nerstian distribution of cationic dyes. Biophys J 53:785–794
188. Chen LB (1988) Mitochondril membrane potential in living cells. Annu Rev Cell Biol 4:155–181
189. Huang M, Camara AKS, Stowe DF, Qi F, Beard DA (2007) Mitochondrial inner membrane electrophysiology assessed by Rhodamine-123 transport and fluorescence. Ann Biomed Eng 35:1276–1285
190. Pelin DS, Kasamo K, Brooker RJ, Slayman CW (1984) Electrogenic H+ translocation by the plasma-membrane ATPase of Neurospora- studies on plasma membrane vesicles and reconstituted enzyme. J Biol Chem 259:7884–7892
191. Kiehl R, Hanstein WG (1984) ATP-dependent spectrl response of oxonol VI in an ATP-Pi exchange complex. Biochim Biophys Acta 766:375–385
192. Apell HJ, Bersch B (1987) Oxanol VI as an optical indicator for membrane potentials in lipid vesicles. Biochim Biophys Acta 903:480–494
193. Bashford CL, Chance B, Smith JC, Yoshida T (1979) The behavior of oxonol dyes in phospholipid dispersions. Biophys J 25:63–85
194. Smith JC, Russ P, Cooperman BS, Chance B (1976) Synthesis, structure determination, spectral properties, and energy-linked spectral responses of the extrinsic probe oxonol V inmembranes. Biochemistry 15:5094–5105
195. Waggoner AS, Wang CH, Tolles RL (1977) Mechanism of potential-dependent light absorption changes of lipid bilayer membranes in the presence of cyanine and oxonol dyes. J Membrane Biol 33:109–140
196. Gonzalez JE, Tsien RY (1995) Voltage sensing by fluorescence resonance energy transfer in single cell. Biophys J 69:1272–1280
197. Gonzalez JE, Tsien RY (1997) Improved indicators of cell membrane potential that use fluorescence resonance energy transfer. Chem Biol 4:269–277
198. Molokanova E, Savchenko A (2008) Bright future of optical assays for ion channel drug discovery. Drug Disc Today 13:14–22
199. Loew LM, Bonneville GM, Surow J (1978) Charge shift optical probes of membrane potential. Theor Biochem 17:4065–4071
200. Loew LM (1982) Design and characterization of electrochromic membrane probes. J Biochem Biophys Meth 6:243–260
201. Loew LM, Cohen LB, Dix J, Fluhler EN, Montana V, Salama G, Wu J-Y (1992) A naphthyl analog of the aminostyryl pyridinium class of potentiometric membrane dyes shows consistent sensitivity in a variety of tissues, cells, and model membrane preparations. J Membr Bio 130:1–10
202. Loew LM, Cohen LB, Salzberg BM, Obaid AL, Bezanilla F (1985) Charge shift probes of membrane potential. Characterization Biophys J 47:71–77
203. Montana V, Farkas DL, Loew LM (1989) Dual wavelength ratiometric fluorescence measurements of membrane potential. Biochem 28:4536–4539
204. Portele A, Lenz J, Hofer M (1997) Estimation of membrane potential DF in reconstituted plasma membrane vesicles using a numerical model of oxonol VI distribution. J Bioenerg Biomem 29:603–609
205. Ivashchul-Kienbaum YA (1996) Monitoring of the membrane potential in proteoliposomes with incorporated Cytochrome-c oxidase using the fluorescent dye indocyanine. J Membr Bio 151:247–259
206. Vecer J, Herman P, Holoubek A (1997) Diffusion membrane potential in liposomes: setting by ion gradients, absolute calibration and monitoring of fast changes by spectral shifts of diS-C3(3) fluorescene maximum. Biochim Biophys Acta 1325:155–164
207. Vecer K, Holoubek A, Sigler K (2001) Fluorescence behavior of the pH-sensitive probe carboxy SNARF-1 in suspension of liposomes. Bhotochem Photobiol 74:8–13
208. Rottenberg H (1989) Probe electrochemical gradient in vesicles, organelles and prokaryotic cells. Methods Enzymol 172:63–84
209. Holoubek A, Vecer J, Opekarov'a M, Sigler K (2003) Ratiometric fluorescence measurements of membrane potential generated by yeast plasma membrane H+ -ATPase reconstituted into vesicles. Biochim Biophys Acta 1609:71–79
210. Veatch ER, Mathies R, Eisenberg M, Stryer L (1975) Simultaneous fluorescence and conductance studies of planar bilayer membranes containing a highly active and fluorescence analog of gramicidin A. J Mol Biol 99:75–92
211. Shapiro HM (1994) Cell membrane potential analysis. Methods Cell Biol 41:21–133
212. Shapiro HM (1995) Practical flow cytometry, 3rd edn. Wiley-Liss, Weinheim
213. Muller S, Lofhagen N, Bley T, Babel W (1996) Membrane potential related fluorescence intensity indicates bacterial injury. Microbiol Res 151:127–131

214. Kudo S, Morigaki R, Saito J, Ikeda M, Oka K, Tanishita K (2000) Shear-stress effect on mitochondrial membrane potential and albumin uptake in culture endothelial cells. Biochem Biophys Res Commun 270:616–621
215. Salvioli S, Ardizzoni A, Franceschi C, Cossarizza A (1997) JC-1 but not DiOC6(3) or rhodamine 123, is a reliable fluorescent probe to assess delta psi changes in intact cells: implications for studies on mitochondrial functionality during apoptosis. FEBS Lett 411:77–82
216. Ahem CA, Horn R (2005) Focused electric field across the voltage sensor of potassium channels. Nauron 48:25–29
217. Miesenbock G, Angelis DA, Rothman JE (1998) Visualizing secretion and synaptic transmission with pH-sensitive green fluorescent protein. Nature 394:192–195
218. Miyawaki A, Llopis J, Heim R, McCaffery JM, Adams JA, Ikura M, Tsien RY (1997) Fluorescent indicators for Ca2+ based on green fluorescent protein and calmodulin. Nature 388:882–887
219. Roorda RD, Hohl TM, Toledo-Crow R, Miesenbock G (2004) Video-rate nonlinear microscopy of neuronal membrane dynamics with genetically encoded probes. J Neurophysiol 92:609–621
220. Sakai R, Repunte-Canonigo V, Raj CD, Knopfel T (2001) Design and chrcterization of a DNA-encoded, voltage-sensitive fluorescent protein. Eur J Neurosci 13:2314–2318
221. Siegel MS, Isacoff EY (1997) A genetically encoded optical probe of membrane voltage. Neuron 19:735–741
222. Salzberg BM, Grivald A, Cohen LB, Davila HV, Ross WN (1977) Optical recording of neuronal activity in an invertebrate central nervous system: simultaneous minitoring of several neurons. J Neurophysiol 40:1281–1291
223. Mannuzzu LM, Moronne MM, Isacoff EY (1996) Direct physical measure of conformational rearrangement underlying potassium channel gating. Science 271:213–216
224. Cha A, Bezanilla F (1997) Characterizing voltage-dependent conformational changes in the Shaker K+ channel with fluorescence. Nuron 19:1127–1140
225. Chanda B, Bezanilla F (2002) Tracking voltage-dependent conformational changes in skeletal muscle sodium channel during activation. J Gen Physiol 120:629–645
226. Schonherr R, Mannuzzu LM, Isacoff EY, Heinemann SH (2002) Conformational switch between slow and fast gating modes: allosteric regulation of voltage sensor mobility in the EAG K+ channel. Neuron 35:935–949
227. Aggarwal SK, MacKinnon R (1996) Contribution of the S4 segment to gating charge in the Shaker K+ channel. Neuron 16:1169–1177
228. Seoh SA, Sigg D, Papazian DM, Bezanilla F (1996) Voltage sensing residues in the S2 and S4 segments of the Shaker K+ channel. Neuron 16:1159–1167
229. Cha A, Bezanilla F (1998) Structural implications of fluorescence quenching in the Shaker K+ channel. J Gen Physiol 112:391–408
230. Asamoah OK, Wuskell JP, Loew LM, Bezanilla F (2003) A fluorometric approach to local electric field measurements in a voltage-gated ion channel. Neuron 37:85–97
231. Peleg G, Lewis A, Linial M, Loew LM (1999) Non-linear optical measurement of membrane potential around single molecules at selected cellular sites. Proc Natl Acad Sci USA 96:6700–6704
232. Pons T, Moreaux L, Mongin O, Blanchard-Desce M, Mertz J (2003) Mechanisms of membrane potential sensing with second harmonic generation microscopy. JBiomedOpt 8:428–431
233. Yan ECY, Liu Y, Eisenthal KB (1998) New method for determination of surface potential of microscopic particles by second harmonic generation. J Phys Chem B 102:6331–6336
234. Millard AC, Jin L, Wuskell JP, Boudreau DM, Lewis A, Loew LM (2005) Wavelngth- and time dependence of potentiometric non-linear optical signals from styeyl dyes. J Membrane Biol 208:103–111
235. Ben-Oren I, Peleg G, Lewis A, Minke B, Loew LM (1996) Infrared non-linear optical measuremenys i membrane potential in photoreceptor cells. Biophys J 71:1616–1620
236. Bouevitch O, Lewis A, Pinevsky I, Wuskell JP, Loew LM (1993) Probing membrane potential with non-linear optics. Biophys J 65:672–679
237. Dombeck DA, Sacconi L, Blanchrd-Desce M, Webb WW (2005) Optical recording of fast neuronal membrane potential transients in acute mammalian brain slices by second harmonic generation microscopy. J Neurophysiol 94:3628–3636
238. Millard AC, Jin L, Wei MD, Wuskell JP, Lewis A, Loew LM (2004) Sensitivity of second harmonic generation from styryl dyes to transmembrane potential. Biophys J 86:1169–1176
239. Battersby BJ, Trau M (2002) Novel miniaturized systems in high-throughput screening. Trends Biotech 20:167–173
240. Burg TP, Godin M, Knudsen SM, Shen W, Carlson G, Foster JS, Babcock K, Manalis SR (2007) Weighing of biomolecules, single cells and single nanoparticles in fluid. Nature 446:1066–1069
241. Huang Y, Wang XB, Becker FF, Gascoyne PRC (1997) Introducing dielectrophoreses as a new force field for field-flow fractionation. Biophys J 73:1118–1129
242. Wang XB, Yang J, Huang Y, Vykoukal J, Becker FF, Gascoyne PRC (2000) Cell separation by dielectrophoretic field-flow-fractionation. Anal Chem 72:832–839
243. Maita S, Haups U, Webb WW (1997) Fluorescence correlation spectroscopy: diagnostics for sparse molecules. Proc Natl Acad Sci USA 94:11753–11757
244. Pope AJ, Haupts UM, Moore KJ (1999) Homogeneous fluorescence readouts for miniaturized high-throughput screening: theory and proctice. Drug Discov Today 4:350–362
245. Fitchen N, O'Shea P, Williams P, Hardie KR (2003) Electrostatic sensor for identifying interactions between peptides and bacterial membranes. Mol Immunol 40:407–411
246. Bashir R (2004) BioMEMS: state-of-the-art in detection, opportunities and prospects. Adv Drug Deliv Rev 56:1565–1586
247. Chovan T, Guttman A (2002) Microfabricated devices in biotechnology and biochemical processing. Trends Biotechnol 20:116–122
248. Dai WG, Pollock-Dove C, Dong LC, Li S (2008) Advanced screening assays to rapidly identify solubility-enhancing formulations: high-throughput, miniaturization and automation. Adv Drug Deliv Rev 60:657–672